Penerbit Akademia Baru

Journal of Advanced Research in Fluid Mechanics and Thermal Sciences

Journal homepage: www.akademiabaru.com/arfmts.html
ISSN: 2289-7879

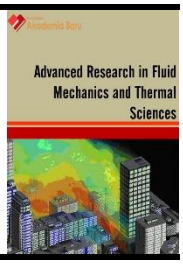

Numerical Simulation for The Forward Flight of the Tri-copter Using Virtual Blade Model

Open Access

Doan Kim Khanh Tran[1], Khanh Nguyen[2], Thi Hong Hieu Le[1,*], Ngoc Hien Nguyen[3]

[1] Department of Aerospace Engineering, Faculty of Transportation Engineering, Ho Chi Minh City University of Technology, Vietnam
[2] Department of Smart Vehicle Engineering, Konkuk University, Republic of Korea
[3] Department of Mathematics, RMIT University, Australia

ARTICLE INFO

Article history:
Received 27 August 2019
Received in revised form 20 October 2019
Accepted 24 October 2019
Available online 15 March 2020

ABSTRACT

This paper presents the process of implementing numerical simulation for a tri-copter in forward flight using the open source code OpenFOAM with the library of Virtual Blade Model (VBM). The tri-copter has 0.75-meter radius and 15-Newton weight. Its propulsion system consists of three two-blade propellers typed XOAR PJP-T-L 1245 with12-inch diameter and 4.5-inch pitch. In the first part, the aerodynamic performance of the tri-copter's frame (not including the propellers) is investigated at the range of angle of attack from -12 degree to 12 degree by simulation in OpenFOAM. Secondly, these force coefficients are exploited in the analytical approach based on the Blade Element Theory (BET) to determine the rotor disk plane angle and the tri-copter's frame angle for steady, level, forward flight at 15-m/s. Finally, after obtaining the relative angle of -2 degree between the rotor tip-path-plane and the tri-copter's frame, the simulation for the tri-copter in forward flight including three rotor disks rotating at 4732-RPM will be carried out through the *rotorDisksource* library of the open source code OpenFOAM. A steady, incompressible solver with k-ω SST turbulence model is applied in the *simple Foam* algorithm. The aerodynamic forces and the dynamic fields surrounding the tri-copter will be discussed in detail, while the effect of tri-copter's frame on rotor operation will also be considered. Moreover, the results of thrust from each propeller from simulation are compared to that of analytical BET method and that of propeller performance provided by the manufacturer. This comparison proves rational of using virtual disk to replace real propeller in the CFD simulation.

Keywords:
tri-copter; forward flight; VBM; rotorDisksource; OpenFOAM

1. Introduction

Nowadays, the interest of UAV (Unmanned Aerial Vehicle) is advancing very quickly in both civilian and military usages. The UAVs have great potential in many areas such as: agriculture, inspection, energy and entertainment. The most popular type of UAVs is drone, including quad-rotor and tri-copter. Tri-copter and other multi-rotors are capable of Vertical Take-Off and

*Corresponding author.
E-mail address: honghieu.le@hcmut.edu.vn (Thi Hong Hieu Le)

https://doi.org/10.37934/arfmts.67.1.132

Landing (VTOL) and hovering flight [1]. So, they are known as smart air vehicles with a wide range of application; for example, UAVs are used for searching and rescuing activities, inspection in agricultural season, merchandise delivery service. In this paper, we will concentrate on the tri-copter's aerodynamic behaviors by the numerical method. This tri-copter model of 0.75 meter-radius and 15 Newton-weight with three rotor propellers typed XOAR PJP-T-L 1245 used as the propulsion system is illustrated in Figure 1.

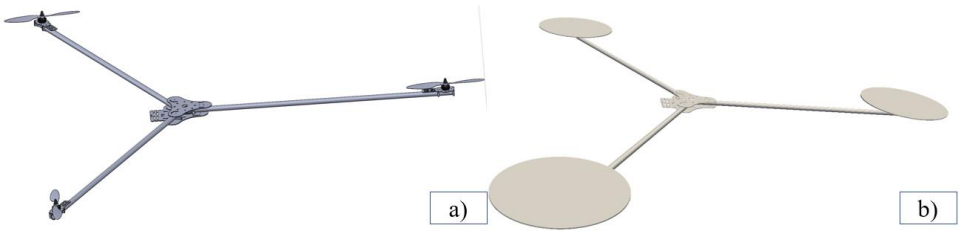

Fig. 1. a) The tri-copter model b) The tri-copter model using Virtual Blade Model

To simulate or calculate the airflow characteristics through tricopter's rotors, different methods have been developed. In analytical approach, BET or Blade Element Momentum Theory (BEMT) is used. In numerical approach, there are several common numerical methods such as Moving Reference Frame method (MRF) or Virtual Blade Model (VBM). In this paper, the rotor disks will be modeled by virtual blade method, which allows investigating aerodynamic performance of the rotors. It does not require the three-dimensional model of rotors. The virtual disk is also combined with momentum sources which are calculated by BET [2,3]. VBM just requests the rotor's geometric parameters such as the geometric angles at local blade element, the sectional chord length and airfoil types distributed along the blade from the root to tip. In addition, turbulence model and airflow conditions will be also declared for VBM. As for that reason, the cell numbers of mesh domain and the execution time are significantly decreased. According to Wahano's report [4], the VBM could be one of the efficient methods to evaluate the aerodynamics of rotor blades in different flight modes. His study focus on the helicopter model in forward flight, the rotor was modeled as the virtual disk of 0.914-meter diameter. The fact that his simulation result shows good agreement with that of experiment for the case of helicopter is a source of reliable reference for the research group to carry out the simulation for the tri-copter.

The purpose of this paper is to apply *rotorDisksource* library in OpenFOAM and VBM method to simulate the airflow characteristics of three rotors on the tri-copter in forward flight mode. This study completes the simulation for three popular flight modes of tri-copter including hover, climb and forward [5,6]. Khanh NGUYEN *et al.,* [5] presented the computational study for the same tri-copter model in hovering by the VBM approach in OpenFOAM. Simulation for the forward flight of tri-copter is implementing by addressing two main problems: firstly, determining two position angles of tri-copter in forward flight by the Blade Element Theory (BET) and secondly, simulating the tricopter in OpenFOAM software. The contents of this paper can be listed as follows. In Section 2, the methodology of this research is presented. In Section 3, the numerical simulation for tri-copter's frame without three rotors is established to find the drag force in forward flight. The results of this section will be input to resolve a problem in the next section. In Section 4, the analytical method for estimating the rotor and tri-copter's frame positions is presented. The method is based on BET of tri-copter aerodynamics for steady, level flight. In Section 5, the numerical approach will be discussed in detail. It includes propeller's characteristics, mesh domain, turbulence model, boundary conditions and numerical results. Eventually, some conclusions and recommendations are addressed in Section 6.

2. Methodology

In this research, the process for tri-copter in forward flight simulation is established through three-step-solving approach. Firstly, the drag of tri-copter's frame was calculated by CFD simulation. The simulation results of the tri-copter's frame without propellers not only provides drag force variation in the range of angle of attack for the determination of the positional angles between the rotor plane and the frame, but also check the validity of the computational domain, the meshing convergence and the algorithm for the implementation of the complete tri-copter model with propeller in forward flight by OpenFOAM software. Secondly, based on BET and phenomenon of helicopter in real case, the positions of rotor disks and tri-copter's frame are determined. These values depend on the tri-copter take-off weight, the forward speed, the propeller features such as distribution of chord-length, twist angles and the airfoil types from root to tip. Finally, after having the 3D CAD model of the tri-copter with virtual disk representing the three rotors in the computational rectangular shape domain, the numerical simulation for tri-copter in forward flight is implemented in OpenFOAM software using rotorDisksource library. The tri-copter is simulated with 15-m/s of forward speed and using simpleFoam algorithm. The VBM method is used to describe the real propeller of tri-copter.

All the simulation results of the tri-copter in Section 3 and Section 5 will be verified by grid independence results of the two structured meshes, including: a fined mesh and a coarse mesh. More specifically, section 3.3.4 presents the verification of the simulation of the tri-copter's frame alone (without propellers) by comparing the results obtained from two structured meshes. To check globally the drag coefficient, the tri-copter's frame is assimilated with the cylinder of similar diameter and length at the same Reynolds number. Regarding the full model of tri-copter with propellers operating at 4732-RPM, section 5.5.4 presents the validation of the simulation results by comparing the overall thrust and drag achieved from two mesh structures with that of the analytical method based on BET and data thrust from the propellers' manufacturer.

3. Drag of Tri-Copter's Frame Without Three Rotors

The drag of the tri-copter's frame without three rotors is one of the important input conditions for the next problem to find the angles of tri-copter in forward flight mode, described in Section 4. In this research, the lift of the tri-copter's frame is assumed to be very small and negligible because the parts of tri-copter include two plates and three cylinder arms. This drag (D_{frame}) can be obtained from many different methods: experiment in wind tunnel or implement numerical simulation. In this paper, the numerical simulation is used to calculate the drag for the tri-copter's frame without three rotors. It will be implemented in the OpenFOAM software.

3.1 Problem Identification

Tri-copter without three rotors has the following basic parameters as shown in Table 1 and Figure 2.

Table 1
Tri-copter specifications

Parameter	Value	Unit
Arm length (L_{ref})	0.75	m
Diameter of tri-copter's arm (l_{ref})	0.016	m
Reference area (frontal area - S_{ref})	$0.016 \times 1.33 = 0.02$	m^2

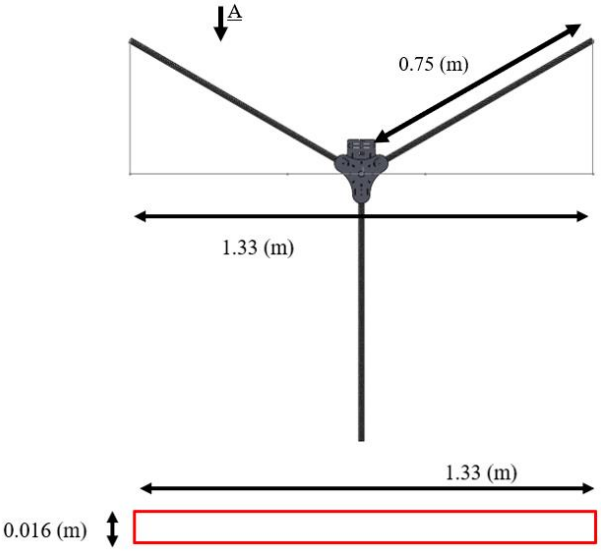

Fig. 2. Reference area for tri-copter model, looking from A

The drag of tri-copter's frame will be calculated at the angle of attack (α_{frame}) from -12 degree to 12 degree at Reynolds number

$$Re = \frac{\rho U_{\inf} l_{ref}}{\mu_{air}} = \frac{1.225 \times 15 \times 0.016}{1.802 \times 10^{-5}} = 16315 \quad (1)$$

Simulating for tri-copter's frame at angle of attack only from -12 degree to 12 degree because this range is estimated value when tri-copter flies in forward flight as shown in Figure 3. Also, the tri-copter was built and experienced some flight tests. The Euler angles was measured by the sensors in the control board. It is observed that the maximum pitching angle (or α_{frame}) in forward flight is approximately -12 degree [7].

Fig. 3. Angles of tri-copter's frame are investigated

3.2 Geometry and Mesh Configuration for Tri-Copter's Frame Simulation

The computational domain is a rectangular shape [8] with dimensions referenced by a value Z = (0.75 + 0.15) x 2 = 1.8-m (0.75-m is tri-copter's arm length and 0.15-m is radius of propeller). Also, it will be divided into three boundary regions including: inlet, outlet and tri-copter as shown in Figure 4.

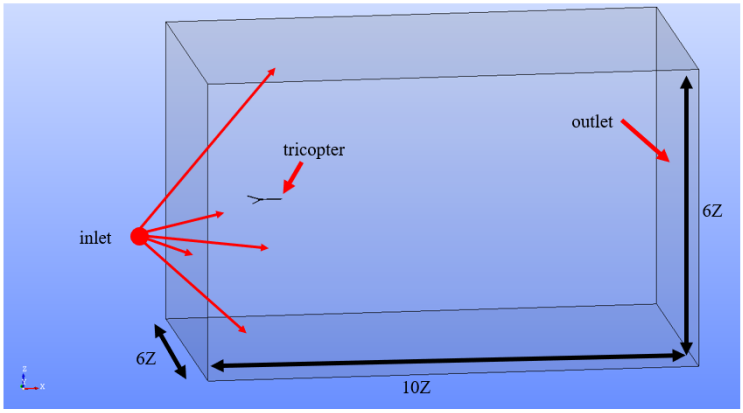

Fig. 4. Computational domain and sizing with respect to parameter Z

In this research, mesh is generated by two softwares. Firstly, Salome tool is used for meshing the rectangular domain, which is defined as a background hexahedral mesh (as shown in Figure 6). Secondly, *snappyHexMesh* tool of OpenFOAM software is used to refine hexahedral mesh for the tri-copter and three rotors with the desired layers (as shown in Figure 5).

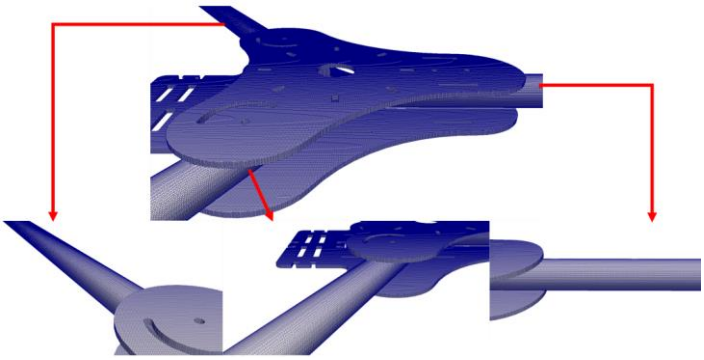

Fig. 5. Mesh domain on tri-copter's frame

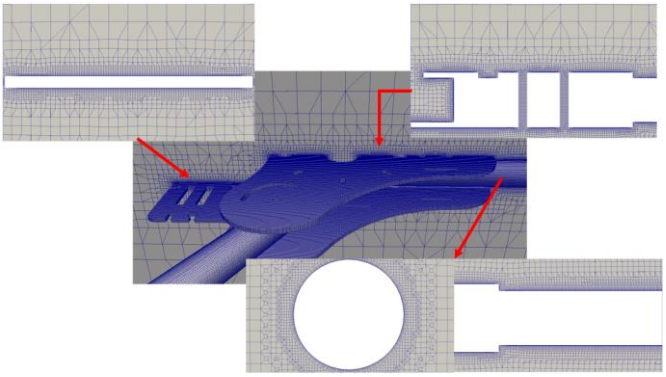

Fig. 6. Mesh domain around tri-copter's frame

Layers around the wall surface are always one of the most important factors for the CFD analysis. It means that the normal distance from the first layer to the wall surface must be considered carefully. This factor is denoted by non-dimensional value y^+ [9]. The simulation is analyzed in a low Reynolds turbulence model integrated the wall function to solve the near wall region (k-ω SST). That requires the first cell center needed to be placed at the viscous sublayer. That means the y^+ value must be one [10]. However, the setting of y^+ value equals one during mesh generation

lead to the extremely thin first cell, that the mesh quality is detected illegal faces. So, y^+ value was chosen 2, which corresponding approximately to the first layer thickness of 2.9 x 10^{-5} m.

Figure 7 shows the y^+ value on tri-copter's frame after finishing the simulation. Most of y^+ valueon tri-copter's frame is less than 1, average value of 0.68 for whole tri-copter. The minimum value of y^+ is 0.12 and the maximum value is 25.87.

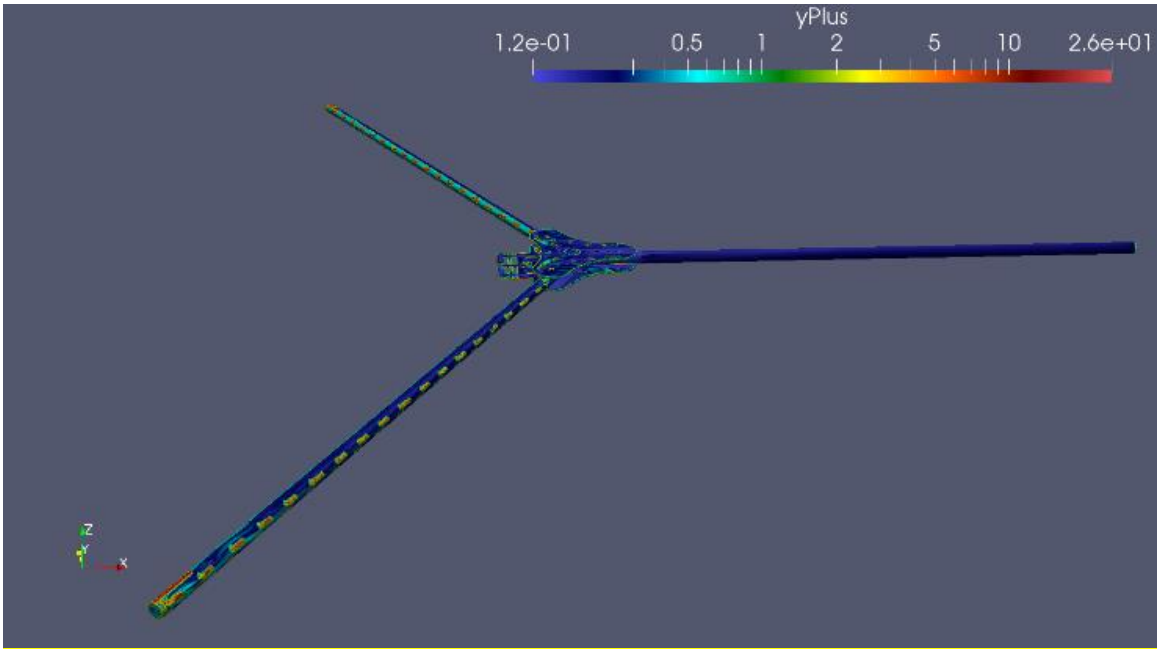

Fig. 7. Distribution of y^+ value on the tri-copter's frame

3.3 Results for Drag of Tri-Copter's Frame

3.3.1 Residual convergence for tri-copter's frame simulation

The simulation is performed for 15-m/s of forward velocity with the convergence criteria of 10^{-5}. For under relaxation factors, 0.3 was used for the pressure field. All other field factors were set to 0.6. At the 0 degree of angle of attack, the convergence was obtained after 7000th iteration. Two structured meshes is built at this stage: a fined mesh of 13 million cells and a coarse mesh of 10 million cells.

The settings for the turbulence model and boundary conditions is presented in Section 5 - the numerical simulation for tri-copter with three rotors in forward flight. These two simulation problems have the same property of airflow and boundary conditions. Therefore, the settings in OpenFOAM software will be also the same.

From the residual curves in Figure 8, despite the fact that the convergence criteria is set 10^{-5}, some variables achieved this value such as turbulence specific dissipation rate - ω, turbulent kinetic energy - k and velocity - U_x while pressure - P, velocity components - U_y, U_z stabilize between 10^{-3} and 10^{-4}. It seems unfeasible to obtain the desired accuracy for these three latter variables including P, U_y and U_z. This is possibly due to some insufficient grid quality relating to the first layer thickness y^+ on the solid part of the tri-copter as mentioned in section 3.2. However, the validation results presented in section 3.3.4 shows reasonable overall drag coefficients. The flow fields exploited from the simulation results of the airflow over the tri-copter's arm alone at 15-m/s can be considered appropriate, to some extent.

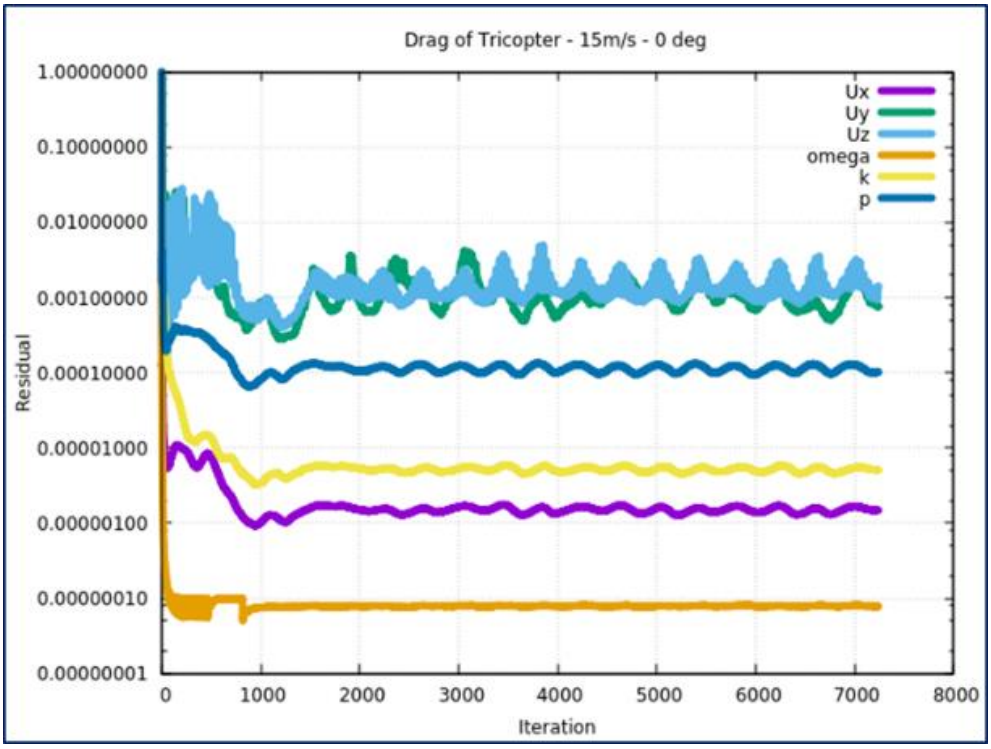

Fig. 8. Residual curves at 0 degree of angle of tri-copter's frame

3.3.2 Simulation results for tri-copter's frame at 0 degree pitching angle

Simulation of the tri-copter's frame without propellers is carried out in the pitching angle ranges from -12 degree to 12 degree. To illustrate the flow fields, the case at 0 degree of angle of attack is chosen for the sake of comparison with the relevant blunt body in the literature. Here, the drag coefficient of tri-copter's frame isC_D = 0.77. In Figure 9 and Figure 10, we see that the fluid velocity increases after going through the arm of the tri-copter, the velocity on the arm of the tri-copter can reach the value equal 20-m/s. Because the arm of the tri-copter is shaped like a cylinder, so the airflow going through the arms will be the same as going through a simple cylinder.

In Figure 11 and Figure 12, these figures represent the velocity vector and the velocity field going through the tri-copter's arm in a section. The fluid velocity increases when passing through the arm due to the linear shape. Moreover, the flow is separated on the front of the tri-copter's arm.

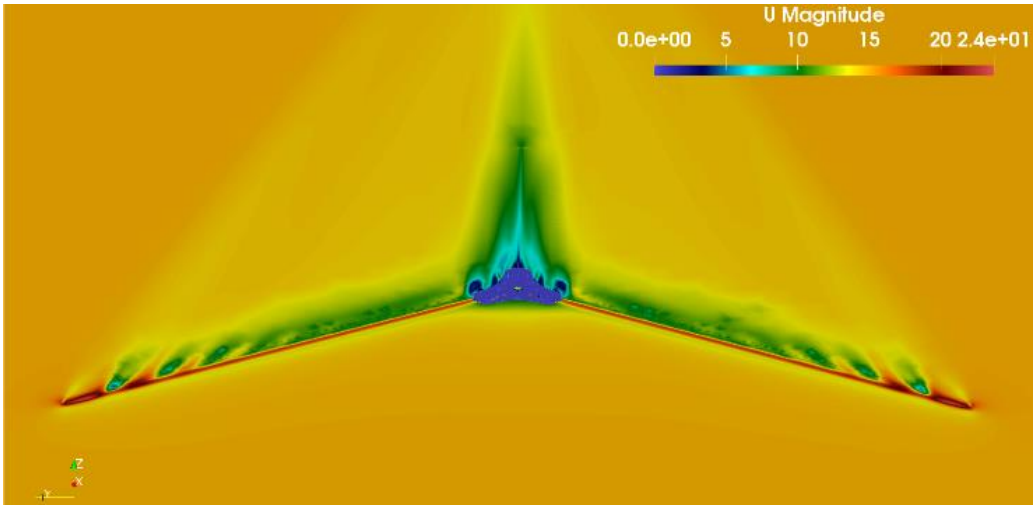

Fig. 9. Velocity field at 0 degree angle of tri-copter's frame (m/s)

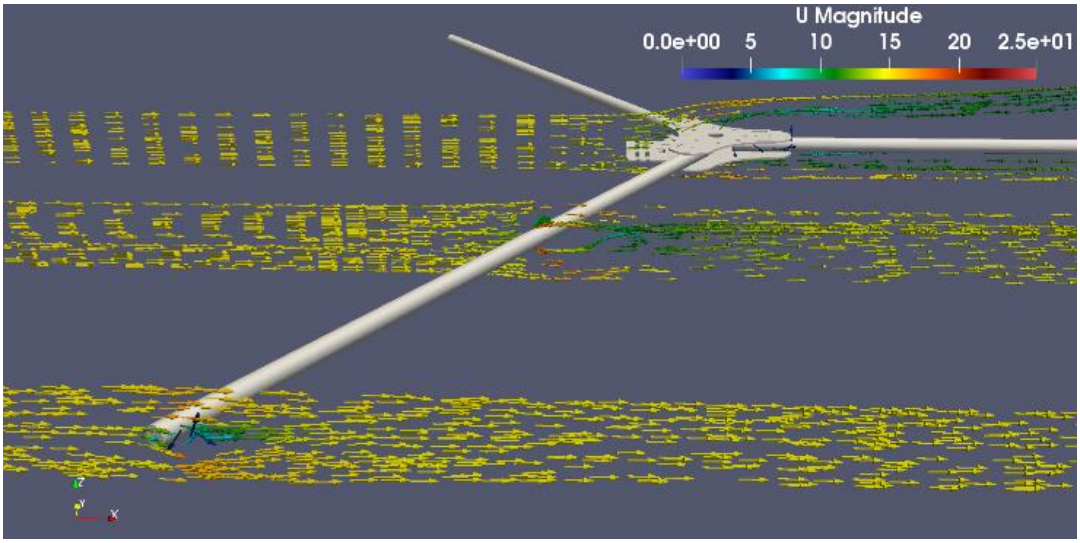

Fig. 10. Velocity vectors through tri-copter's frame (m/s) (α_{frame} = 0 degree)

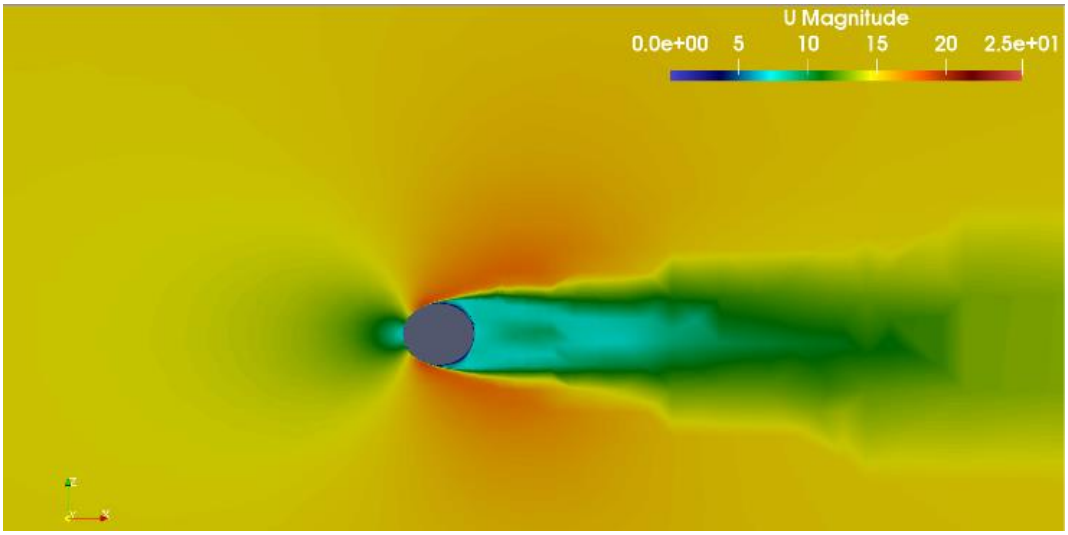

Fig. 11. Velocity field through tri-copter's arm (m/s) (α_{frame} = 0 degree)

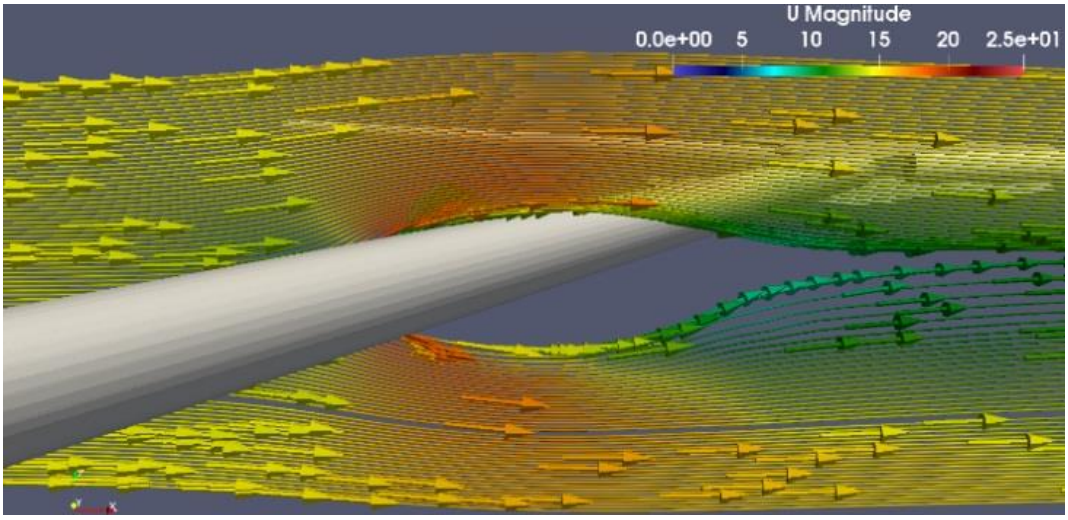

Fig. 12. Streamlines through tri-copter's arm (m/s) (α_{frame} = 0 degree)

Figure 13 demonstrates the gradient pressure on the surface of the tri-copter's frame. In here, the gradient pressure between the front and the rear of the tri-copter's arm is the main cause of the drag for the tri-copter.

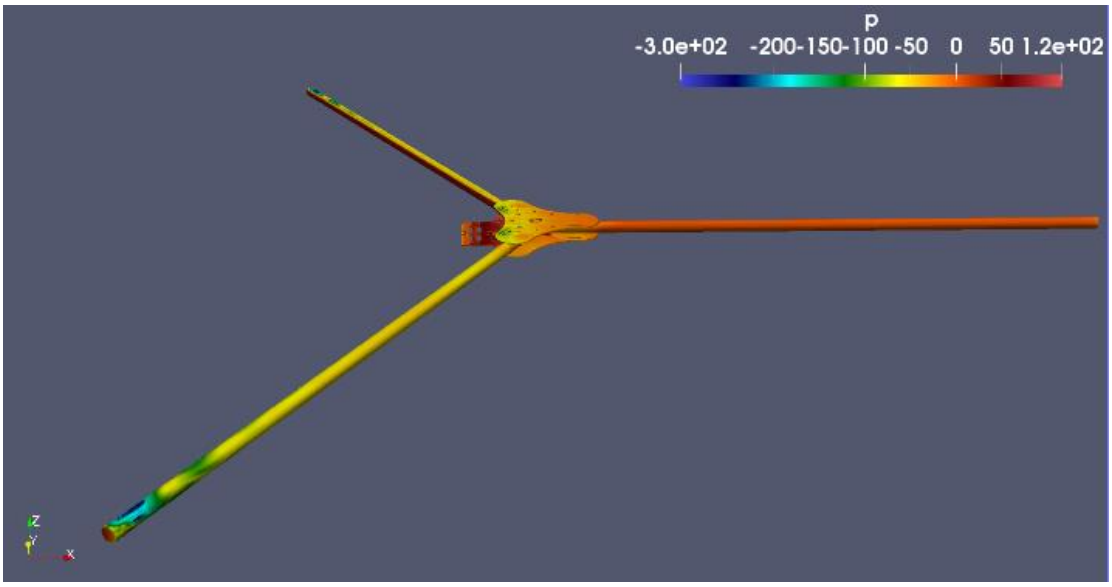

Fig. 13. Pressure field on tri-copter's frame (m^2/s^2) (α_{frame} = 0 degree)

3.3.3 Drag of tri-copter's frame

After performing the simulation for angle of attack range from -12 degree to 12 degree, the drag coefficients of the tri-copter's frame are obtained as shown in Figure 14:

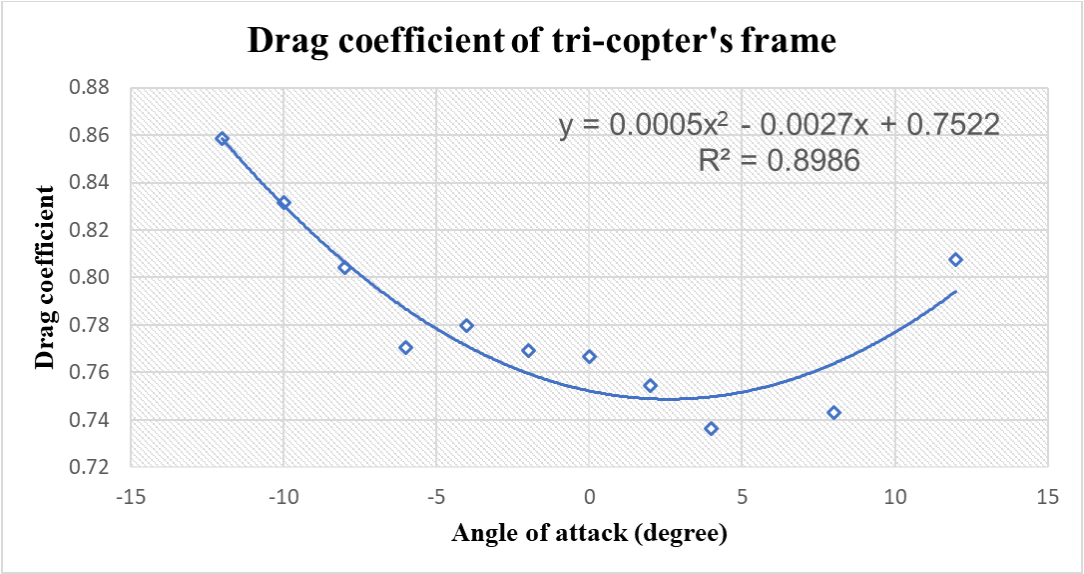

Fig. 14. The chart of drag coefficient according to pitching angles of tri-copter's frame

Finally, the drag of the tri-copter's frame without three rotors will be calculated according to the formula

$$D_{frame} = \frac{1}{2} \times \rho \times U_{\inf}^2 \times S_{ref} \times C_D \quad (2)$$

3.3.4 Results verification for tri-copter's frame simulation

The simulation of the tri-copter's frame will be first verified by grid independence results of the two structured meshes mentioned earlier in section 3.3.1 and summarized in Table 2. Both structured meshes have initial y^+ setting value of 2.

Table 2
Summary of the two structural meshes

Parameter	Mesh 1	Mesh 2
Domain mesh	266 200	200 000
Final grid size	13 235 610	10 641 648
Hexahedral cell number	11 128 691	8 986 555
Percentage of hexahedral cell	84.08 %	84.45 %
Skewness	3.00	3.34
Average non-orthogonality	8.44	8.61
Aspect ratio	27.25	29.95

The "Error" value in Figure 15 is calculated from formula:

$$Error = \frac{C_{D,Mesh1} - C_{D,Mesh2}}{C_{D,Mesh1}} \quad (3)$$

From Figure 15, it can be stated that the difference between two meshes is less than 5% which proves that the drag coefficients are independent of grid scale of the whole computational domain.

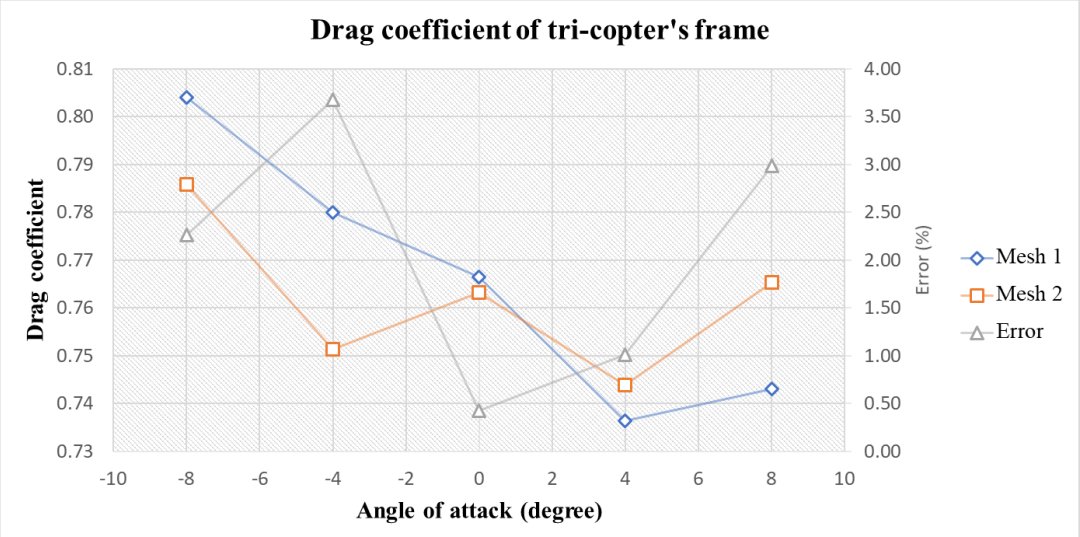

Fig. 15. Drag coefficient of two structural mesh models for tri-copter's frame

On the other hand, the drag coefficients of the tri-copter's frame should be validated with experimental results of similar blunt body in the literature. The most feasibly comparable shape to tri-copter's frame is a cylinder of length 1.33-m and diameter 0.16-m as shown in Figure 2. The drag is created on the tri-copter's frame due to cylindrical arms, mentioned in section 3.3.2. Therefore, with the same value of frontal area, the drag of cylinder can be used to evaluate the simulation results (as shown in Figure 16).

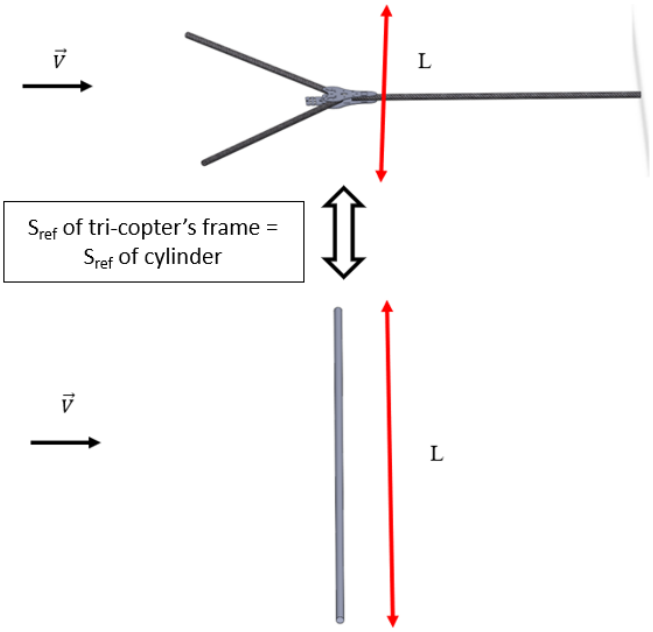

Fig. 16. The cylinder is used to compare to tri-copter's frame

The experimental data of drag for basic cylinder is referenced from the book "Fundamentals of Aerodynamics" of John D. Anderson [11] shown in Figure 17.

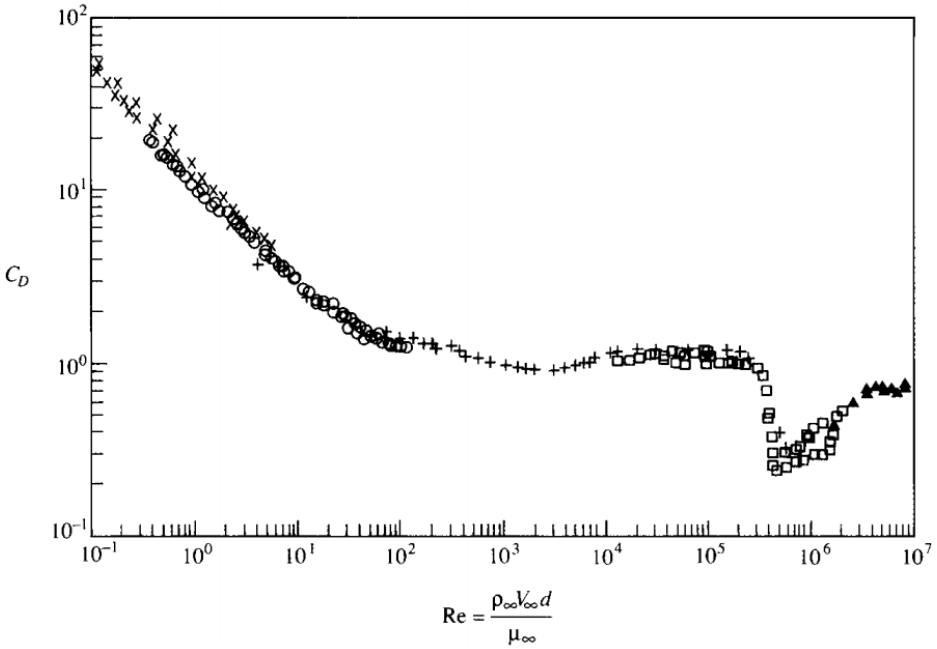

Fig. 17. Variation of cylinder-drag coefficient with Reynolds number [11]

With the Reynolds number approximates 16000, we have the drag coefficient of cylinder is $C_D \approx 0.8$. From simulation, the drag coefficient of tri-copter's frame has value from 0.73 to 0.85. So, the drag coefficients obtained for the tri-copter's frame alone are in good agreement with the case of cylinder of which axis is perpendicular to the air speed.

4. Analytical Approach to Determine the Positions of The Rotor and The Tri-Copter's Frame in Forward Flight

4.1 Problem Definition

In fact, when the helicopter performs forward flight mode, the propeller system creates an angle that called α_{TPP} and the helicopter body also creates another angle that called α_{frame}. Two angles are illustrated in Figure 18.

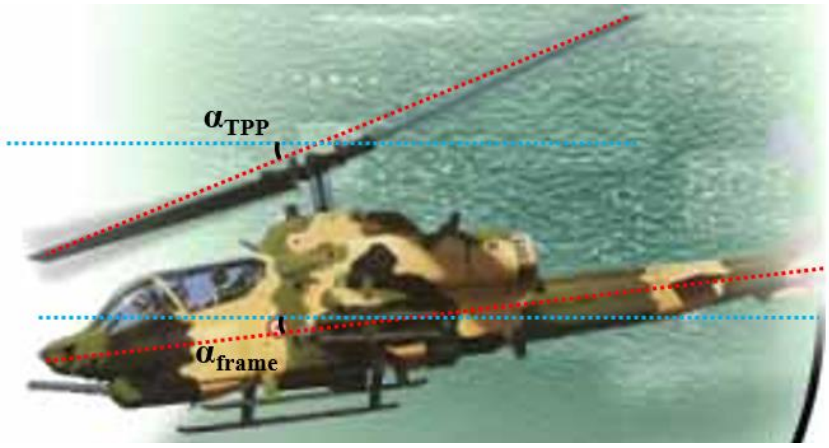

Fig. 18. Helicopter in forward flight mode [12]

Applying phenomena of helicopter to tri-copter in forward flight mode, we consider two main angles of tri-copter (as shown in Figure 19). Firstly, the angle of rotor (α_{TPP} - TPP stands for Tip Path Plane) is an angle between the reference plane of the rotor and the flight direction. Secondly, the angle of tri-copter's frame (α_{frame}) is an angle between the reference plane of tri-copter's body and the flight direction.

These two angles connect with each other through the formula

$$\alpha_{frame} = \alpha_{TPP} - \phi_i \tag{4}$$

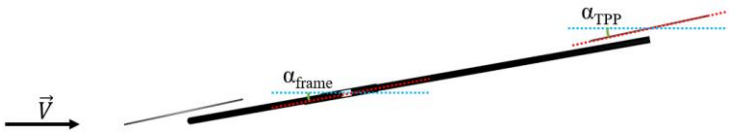

Fig. 19. Angles of tri-copter in forward flight mode

These two anlges are the most important data that have to be calculated before creating the 3D CAD for the simulation problem. To determine the angle of rotor (α_{TPP}), two equilibrium equations need to be set for tri-copter in forward flight, illustrated in Figure 20.

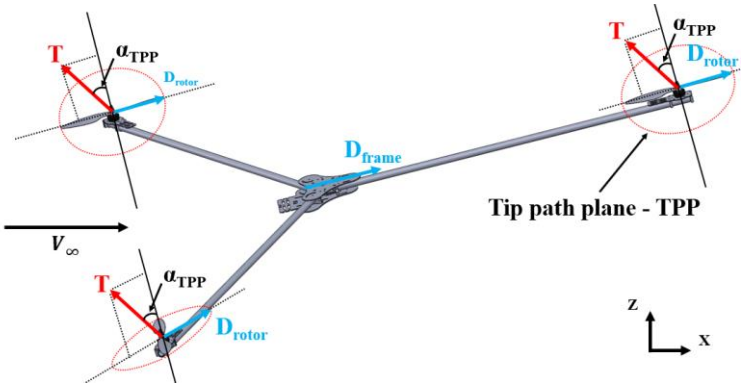

Fig. 20. Force diagram of model in forward flight

In the X direction, we have

$$3T \times \sin(\alpha_{TPP}) = D_{frame} + 3D_{rotor} \tag{5}$$

In the Z direction, we have:

$$3T \times \cos(\alpha_{TPP}) = W \tag{6}$$

From two above equations, the position of rotor is

$$\alpha_{TPP} = \tan^{-1}\left(\frac{D_{frame} + 3D_{rotor}}{W}\right) \tag{7}$$

Therein

i. D_{rotor} is the profile drag of one rotor when operating. This quantity is calculated from Blade Element Theory.
ii. W is the weight of tri-copter. This parameter is constant with value of 15-N.
iii. D_{frame} is the drag of tri-copter's frame without three rotors. This quantity was calculated from the numerical simulation in OpenFOAM software. The results of this parameter is described in Section 3.

4.2 Profile Drag of Rotors

In forward flight mode, propellers of tri-copter also create drag as tri-copter's frame. In order to determine this value, we rely on the Blade Element Theory (BET) [13] (as shown in Figure 21) and the theory for helicopter in forward flight from document "Steady, Level Forward Flight" [12].

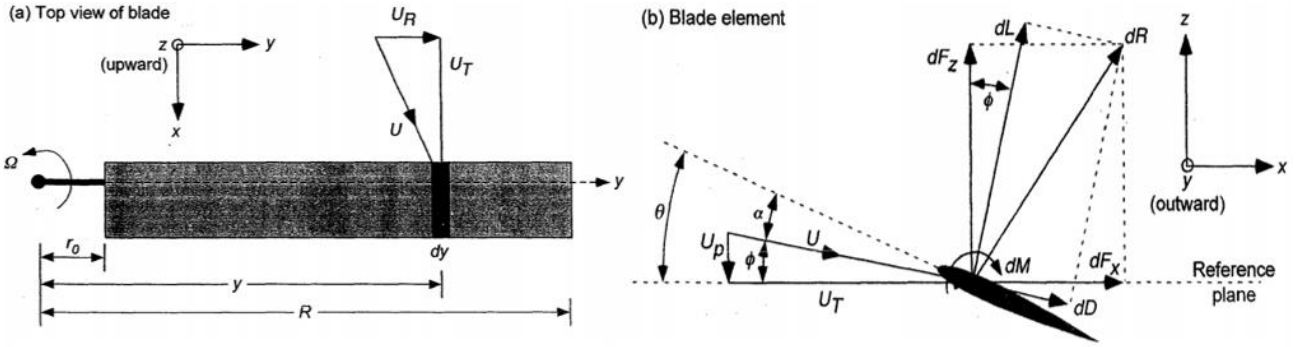

Fig. 21. Incident velocities at a typical blade element [13]

At each section of rotor's blade, the profile drag generated here is

$$dD_{rotor} = dF_x = dL \times \sin(\phi_i) dD \times \cos(\phi_i) \tag{8}$$

With $\phi_i << 0$, the drag created by blades for entire rotor is

$$D_{rotor} = N_b \times \Sigma(dL \times \phi_i + dD) \tag{9}$$

To determine the lift component (dL) and the drag component (dD) in each blade profile, BET calculates through effective angle of attack of blade profile (α_{eff})

$$\alpha_{eff} = \theta_{twist} - \phi_i \tag{10}$$

Induced angle (ϕ_i) is calculated from the velocity components acting on the blade profile: U_P (Out-plane velocity component) and U_T (Tangential velocity component) (as shown in Figure 22).

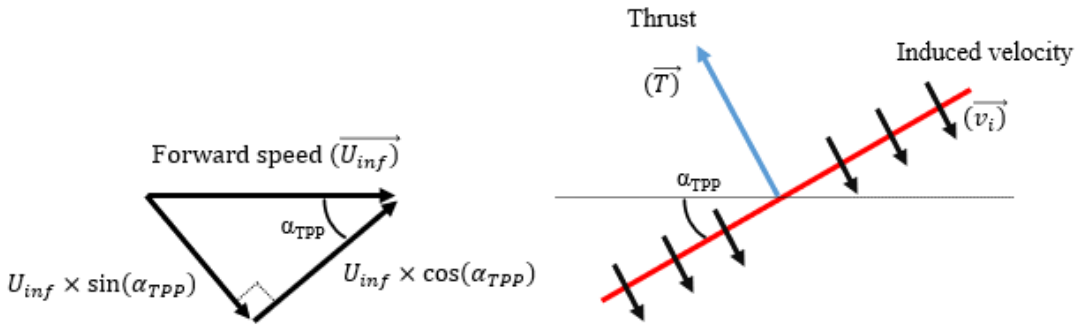

Fig. 22. Cross section of rotor disk plane

$$U_p = \upsilon_i + U_{\inf} \times \sin(\alpha_{TPP}) \tag{11}$$

$$U_T = \Omega r + U_{\inf} \times \cos(\alpha_{TPP}) \tag{12}$$

From BET, detailed formulas for the lift component (dL) and the drag component (dD) are mentioned in Table 3.

Table 3
Application of BET for certain flight mode

Blade Element Theory (BET)		
	$\alpha_{TPP} = 0^0$	$\alpha_{TPP} > 0^0$
	(Hovering flight)	(Forward flight)
U_P	v_i	$v_i(\alpha_{TPP}) + U_{\inf} \times \sin(\alpha_{TPP})$
U_T	$\Omega r + U_{\inf} \times \sin(\psi)$	$\Omega r + U_{\inf} \times \cos(\alpha_{TPP}) \times \sin(\psi)$
ϕ_i	$\frac{U_P}{U_T}$	
α_{eff}	$\alpha_{eff} = \theta_{twist} - \phi_i$	
dL	$0.5 \times \rho \times c \times U^2 \times c_{l,\alpha} \times \alpha_{eff}$	
dD	$0.5 \times \rho \times c \times U^2 \times c_{d,0}$	
dD_{rotor}	$dL \times \phi_i + dD$	

Therein, the profile drag coefficient ($c_{d,0}$) is calculated according to the formula [12]

$$C_{d,0} = \frac{Q \times 8}{\sigma \times \left(1 + \mu^2\right) \times \rho \times \left(\Omega R_{rotor}\right)^2 \times S_{rotor} \times R_{rotor}} \tag{13}$$

4.3 Results for Positions of Rotors and Tri-Copter's Frame

To determine the angle of rotor and the angle of tri-copter's frame, we assume that the initial values of α_{TPP} and α_{frame} are both 0 degree. Then the α_{TPP} value in the next iteration is obtained by calculating values in Eq. (7). Finally, the α_{frame} value in that iteration is achieved from Eq. (4). If calculated error between next two iterations is smaller than convergence criteria, the problem will converge.

In the iteration solution to find the angles of tri-copter, the data of the propeller system from manufacturer [14] should be declared, including

i. RPM value according to the thrust of propeller.
ii. Torque according to the thrust of propeller.
iii. Induced velocity according to the angle of rotor.

The problem will be calculated based on the following diagram, illustrated in Figure 23, with convergence criteria is 10^{-7}.

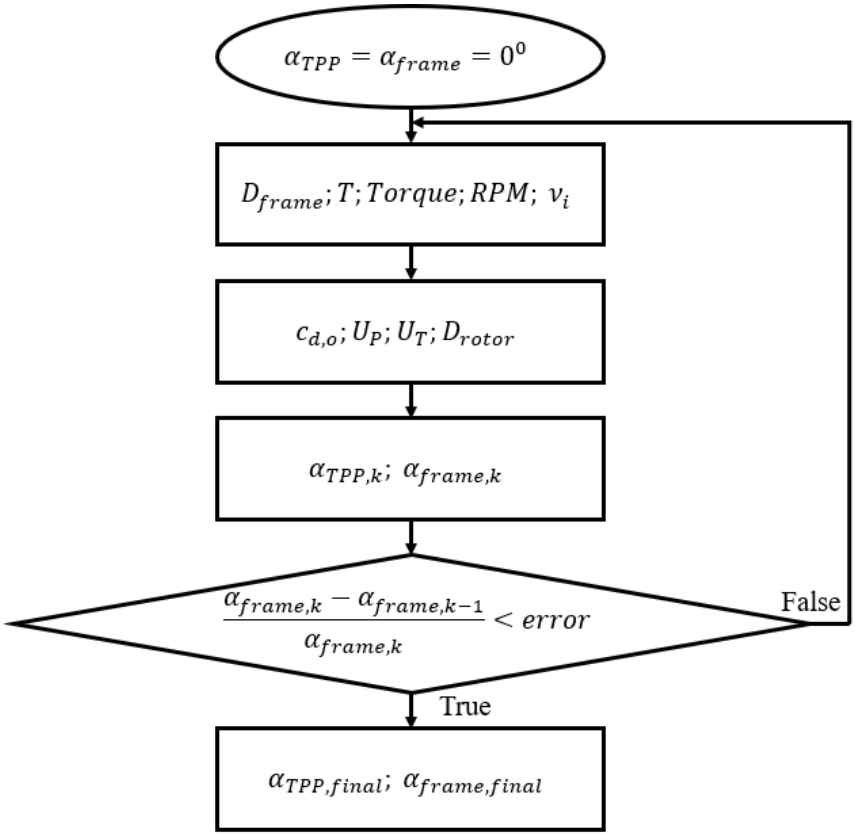

Fig. 23. Calculation process for angles of tri-copter problem

After 13rd iterations, we have some results about tri-copter in forward flight mode as follow (Figure 24).

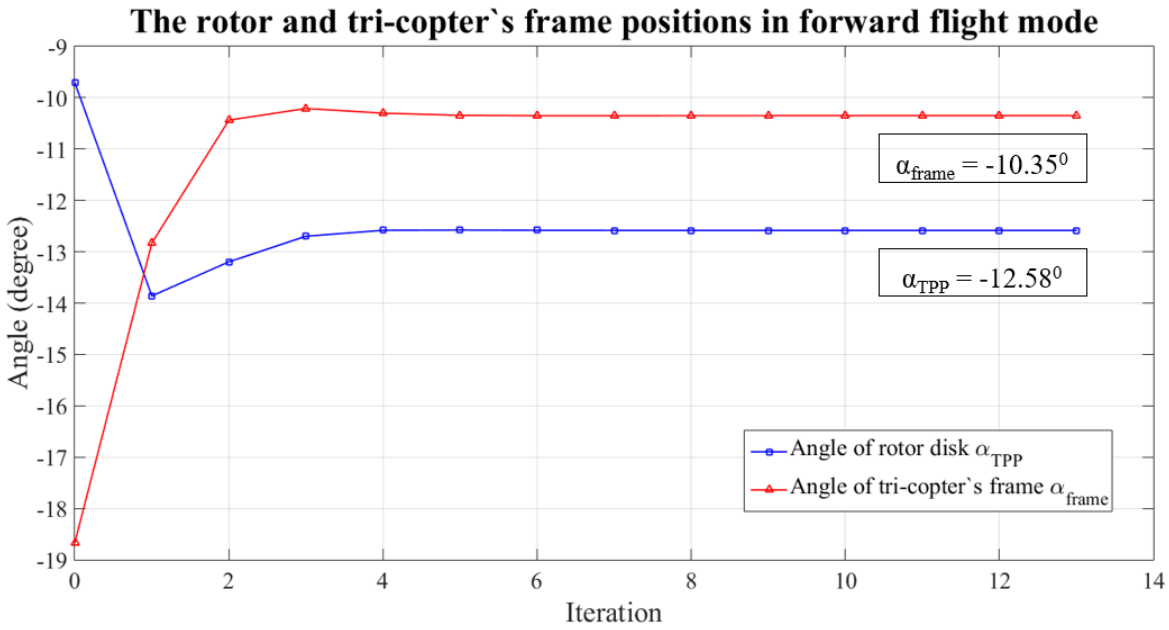

Fig. 24. Results analysis of rotor and tri-copter's frame positions

Beside the values of rotor and tri-coper's frame, the iteration solution also gives some characteristics about tri-copter when it performs at 15-m/s of forward speed. These parameters are described in Table 4. The relative angle of -2 degree between the rotor tip-path-plane and the

tri-copter's frame can be determined for the position of the three rotors and tri-copter's frame which is going to be implemented in the simulation of the tri-copter in forward flight of 15-m/s in OpenFOAM.

Table 4
Results analysis for tri-copter in forward flight using BET

Parameter		Value	Unit
Forward speed		15	m/s
Angle of rotor		-12.58	degree
Angle of tri-copter's frame		-10.35	degree
Rotation speed at one rotor		4732	RPM
Thrust at one rotor		5.03	N
Total drag of tri-copter	Drag force of one rotor	0.28	N
	Drag force of the tri-copter's frame	2.44	

5. Numerical Simulation for Tri-Copter with Three Rotors in Forward Flight Mode

5.1 Description of Rotor Blade Properties

The rotor system used for tri-copter consists of three commercial propellers typed XOAR PJP-T-L 1245. This type of propeller has widely used for multi-rotor vehicles such as quad-rotorortri-copter. It can create a maximum thrust about 15-N at 8000-RPM. The two-blade propellers typed XOAR PJP-T-L 1245 (Figure 25) has the 12-inch diameter (30.48-cm) and the 4.5-inch pitch.

Fig. 25. XOAR PJP-T-L 1245 propeller

To accurately describe the characteristic of propeller, the blade of XOAR PJP-T-L 1245 was divided into 14 sections based on radius length. Parameters to be considered in blade section include: chord length of blade sections, twist angle of blade sections and thickness of blade sections as shown in Figure 26 and Table 5.

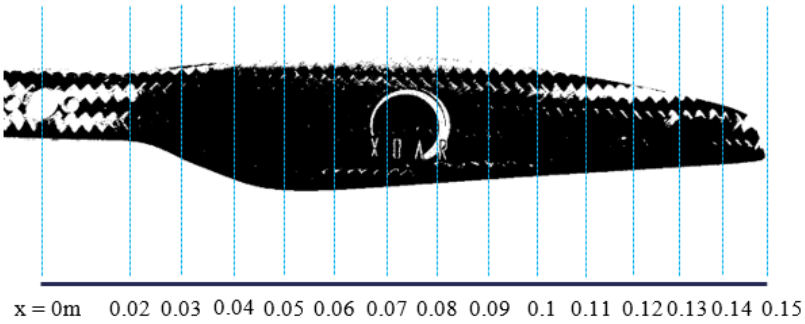

Fig. 26. Blade sections of XOAR PJP-T-L 1245

During the numerical simulation, the blade sections of propeller was referenced as 2D airfoils that created the aerodynamics forces such as lift, drag and moment. These aerodynamic force components were computed according to effective angle of attack (α_{eff}) at each blade section in range from 0 degree to 90 degree. Therefore, the lift coefficient (c_l) and drag coefficient (c_d) of the 2D airfoils at blade sections need to be fully declared. Also, to determine aerodynamic coefficient,

the Reynolds number according to linear velocity at each blade section has to be calculated. It is represented in Table 6.

Table 5
Description of the rotor blade geometry

Position (mm)	Chord length (mm)	Twist (degree)	Thickness (mm)	Ratio of thickness and chord length (%)	Airfoil typed NACA
20	15	27.46	3.3	22	NACA 0012
30	24.3	24.88	4.002	16.47	NACA 0012
40	29.32	22.7	3.66	12.48	NACA 0012
50	30.48	20.89	3.34	10.96	NACA 0012
60	30.3	18.66	3.18	10.5	NACA 0012
70	29.46	16.43	3	10.18	NACA 0012
80	27.86	14.2	2.56	9.19	NACA 0012
90	26.28	11.97	2.18	8.3	NACA 0012
100	24.24	10.38	2	8.25	NACA 0012
110	22.88	9.43	2.16	9.44	NACA 0012
120	19.66	8.74	1.44	7.32	NACA 0006
130	16.88	8.13	1.14	6.75	NACA 0006
140	14.02	7.53	1	7.13	NACA 0006
150	10.4	6.92	0.68	6.54	NACA 0006

Table 6
Reynolds number at each blade section

Position (mm)	Chord length (mm)	Linear velocity (m/s)	Reynolds number	Reynolds number (approximate)	Airfoil typed NACA
20	15	9.91	13 484	15 000	NACA 0012
30	24.3	14.87	24 574	25 000	NACA 0012
40	29.32	19.82	39 535	40 000	NACA 0012
50	30.48	24.78	51 374	50 000	NACA 0012
60	30.3	29.73	61 284	60 000	NACA 0012
70	29.46	34.69	69 516	70 000	NACA 0012
80	27.86	39.64	75 132	75 000	NACA 0012
90	26.28	44.60	79 730	80 000	NACA 0012
100	24.24	49.55	81 713	80 000	NACA 0012
110	22.88	54.51	84 841	85 000	NACA 0012
120	19.66	59.46	79 528	80 000	NACA 0006
130	16.88	64.42	73 973	75 000	NACA 0006
140	14.02	69.37	66 166	65 000	NACA 0006
150	10.4	74.33	52 587	50 000	NACA 0006

The lift and drag coefficient of airfoil profile typed NACA 0012 and NACA 0006 following Reynolds number from Xfoil analytical software are shown in Figure 27 and Figure 28, respectively.

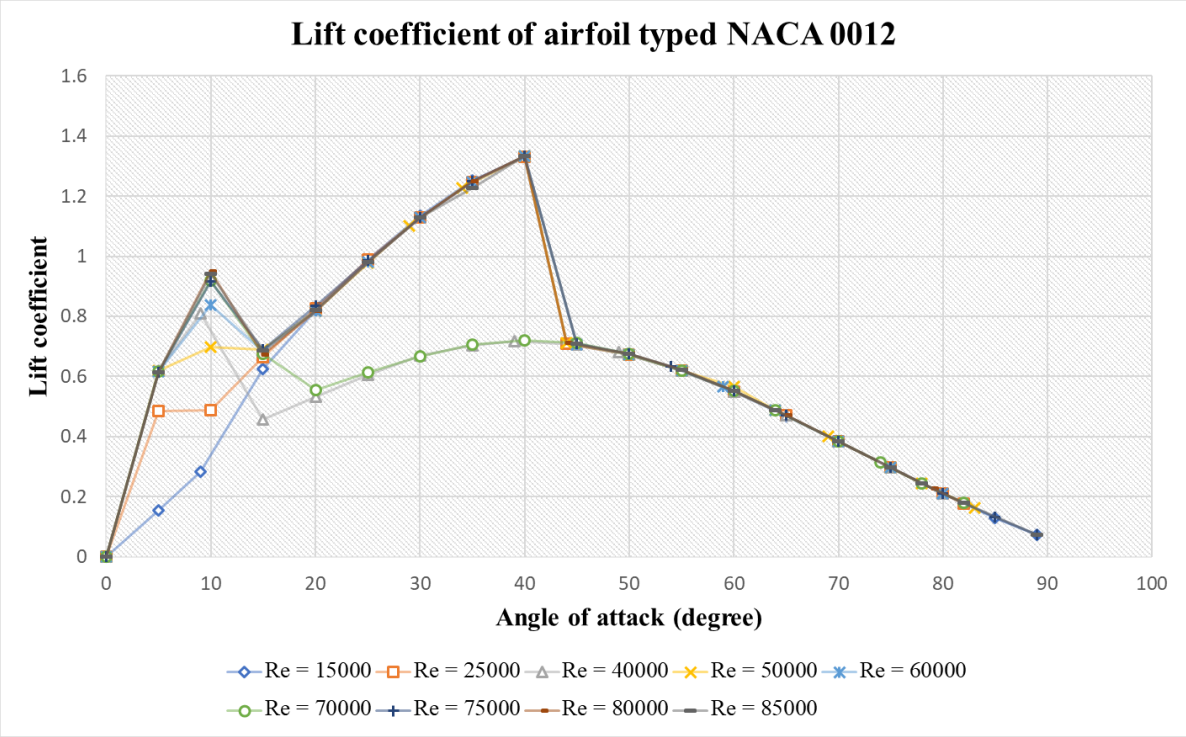

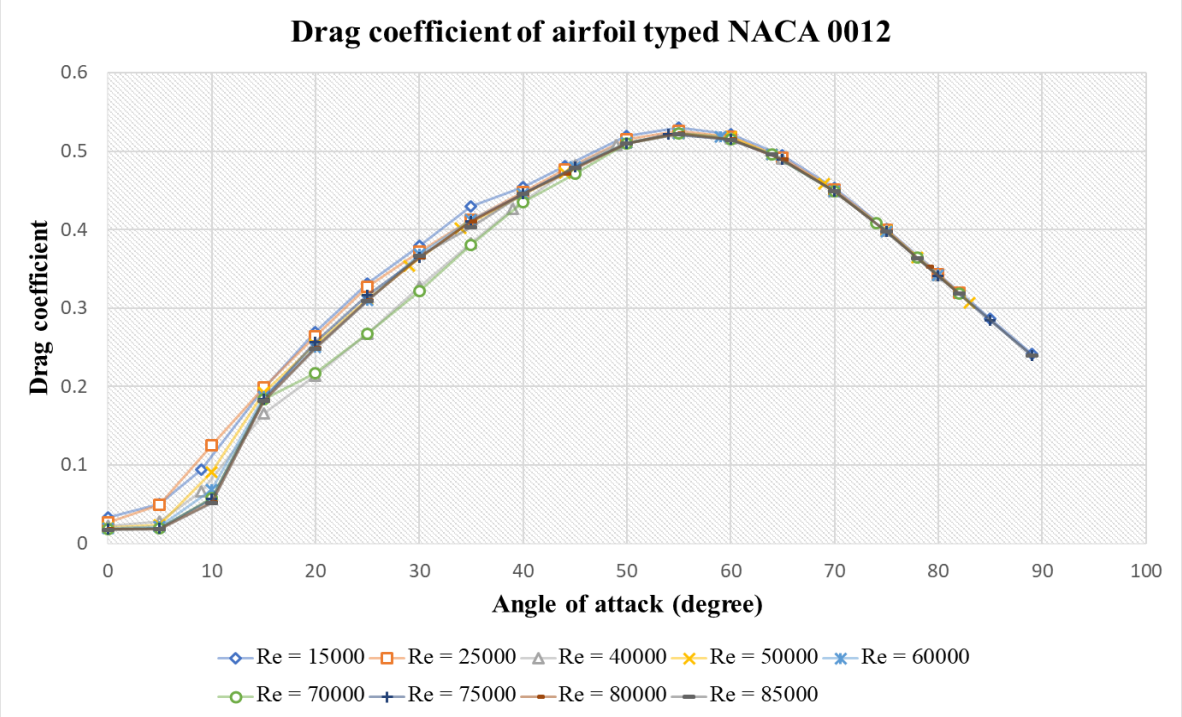

Fig. 27. Lift coefficient and drag coefficient of NACA 0012

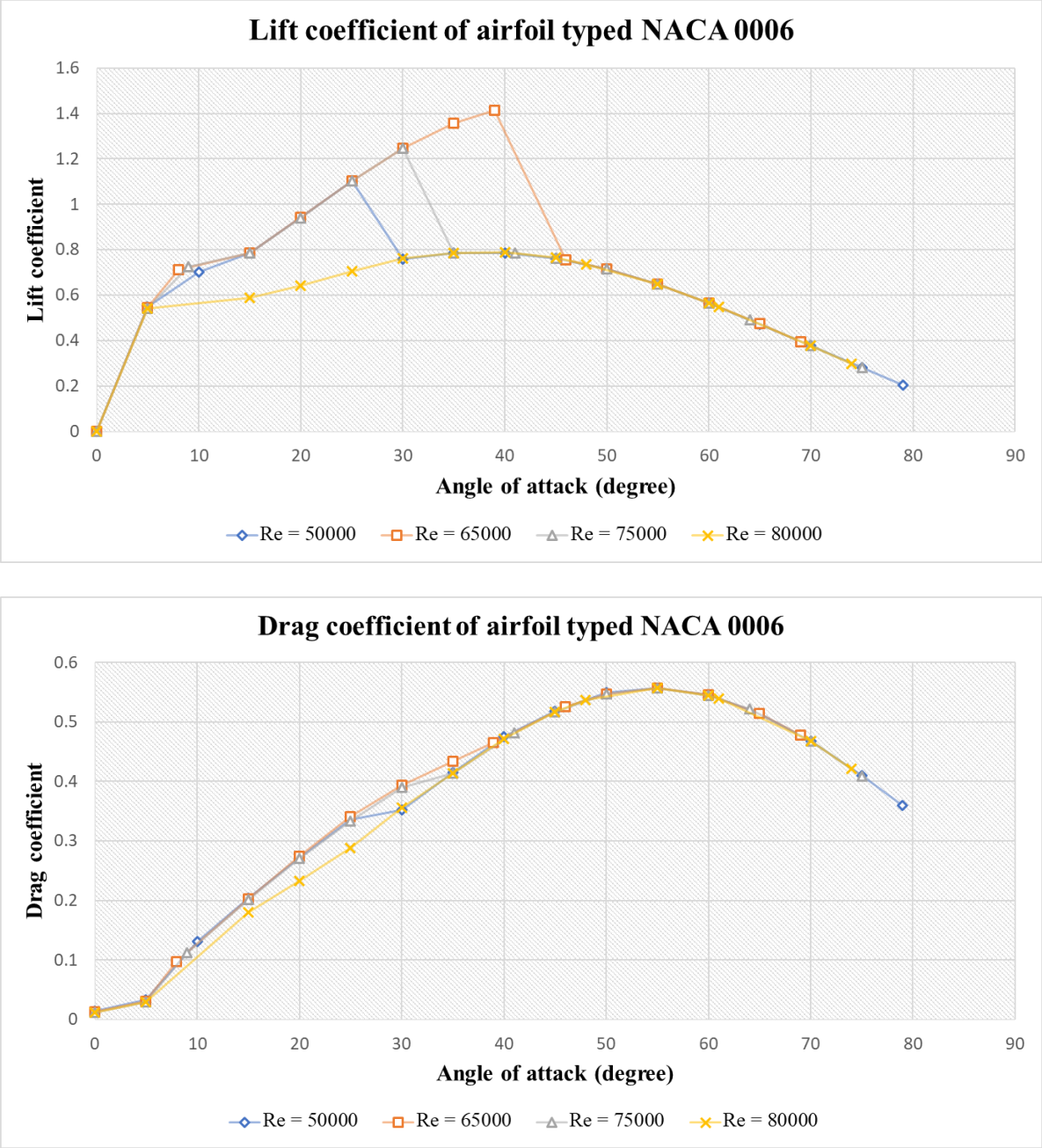

Fig. 28. Lift coefficient and drag coefficient of NACA 0006

5.2 Problem Specification

VBM is a method for replacing the real rotor system with a virtual disk model. In this article, the virtual disk that replaces the XOAR PJP-T-L 1245 has the following dimensions: 0.15-m of radius and 0.003-m of thickness equivalent to 2% of the radius value. In addition, the distance from the tri-copter's frame to virtual disks is also set according to the actual distance (0.03-m) as shown in Figure 29.

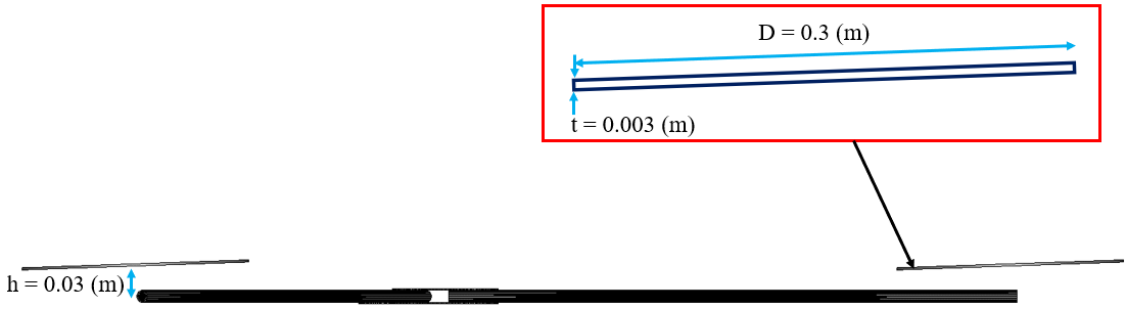

Fig. 29. Characteristics of virtual disk in simulation domain

In forward flight mode (as shown in Figure 30), the positions of rotor and tri-copter's frame depend on its flight speed. In Section 4, with 15-m/s of flight speed, tri-copter has two values.

i. Angle of rotor: α_{TPP} = -12.58 ≈ -12 (degree).
ii. Angle of tri-copter's frame: α_{frame} = -10.35 ≈ -10 (degree).

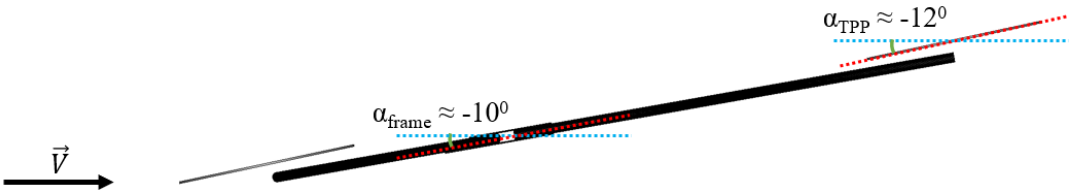

Fig. 30. Positions of rotors and tri-copter's frame in forward flight

However, to facilitate mesh generation for the simulation model, the direction of airflow and tri-copter will be changed as shown in Figure 31 below.

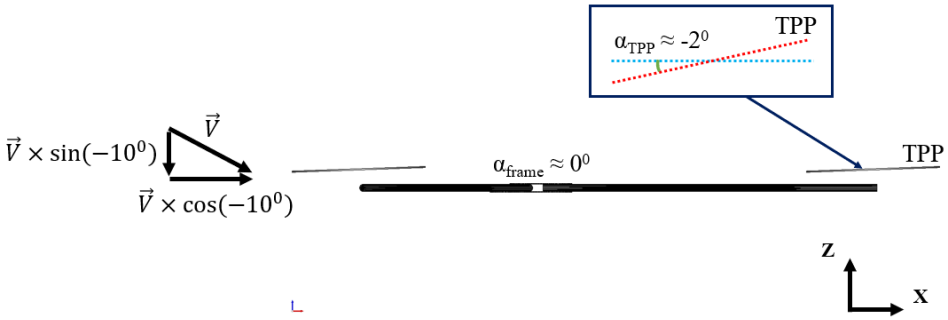

Fig. 31. Positions of rotors and tri-copter's frame in forward flight for simulation model

Rotors are numbered as Figure 32 to identify. In addition, the rotation direction of the rotors system is also shown in Figure 32 with two rotors (Rotor 1 and Rotor 3) having counter-clockwise rotation and another rotor (Rotor 2) having clockwise rotation.

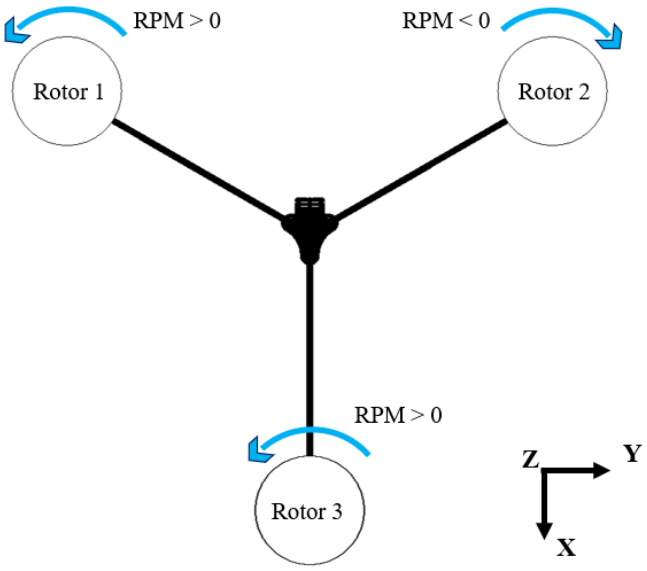

Fig. 32. Rotation direction for rotors of tri-copter

Tri-copter is simulated in the 15-m/s of velocity field with Reynolds number

$$Re = \frac{\rho U_{\inf} l_{ref}}{\mu_{air}} = \frac{1.225 \times 15 \times 0.016}{1.802 \times 10^{-5}} = 16315 \quad (14)$$

5.3 Geometry and Mesh Configuration for Tri-Copter Simulation in Forward Flight

The computational domain of the simulation problem is also a rectangular shape with the same parameters as in Section 3. The dimensions of the calculation domain are referenced by Z = 1.8-m (Figure 33).

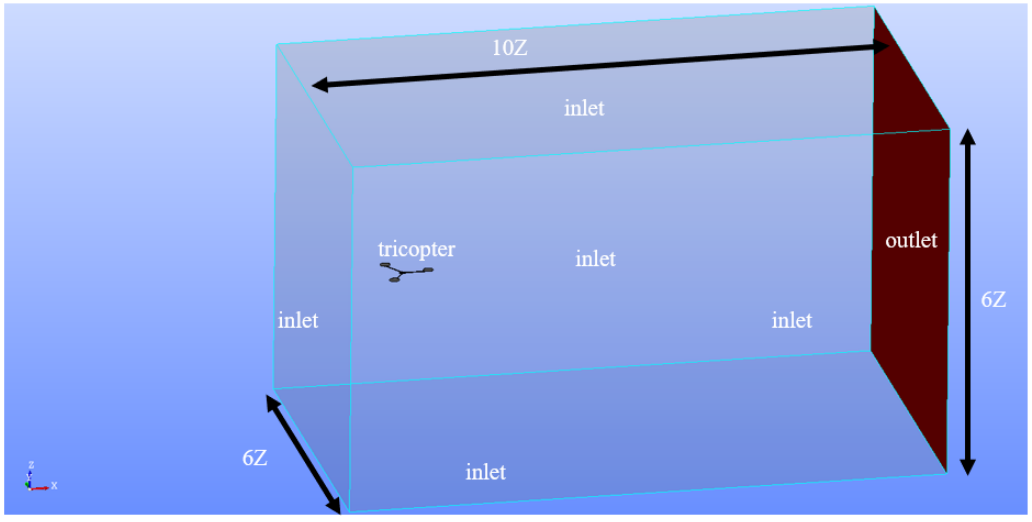

Fig. 33. Computational domain and size

As previously mentioned in Section 3.2, mesh is generated by two tools, Salome and *snappyHexMesh*. At rotor disk, the thickness is only one cell element. In this paper, we choose y^+ value equal 2, so the first layer thickness of mesh generation is 2.9×10^{-5} (m) (Figure 34 - 36).

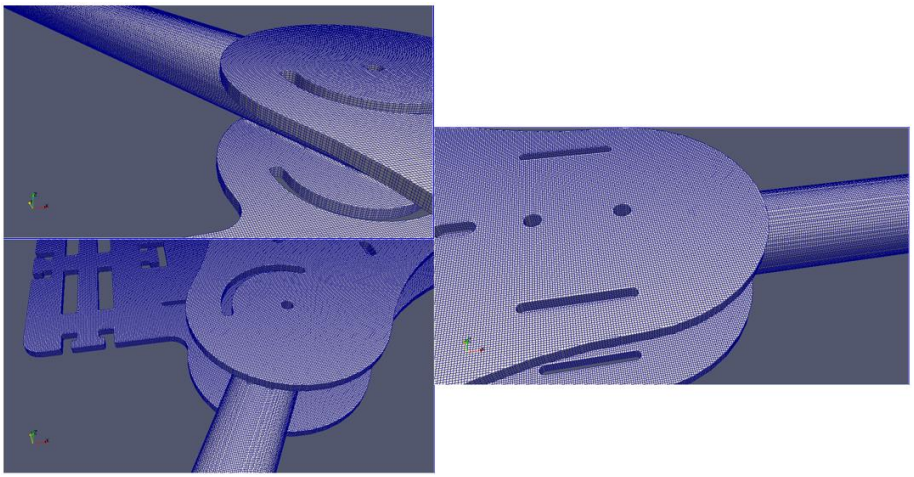

Fig. 34. Mesh generation on tri-copter

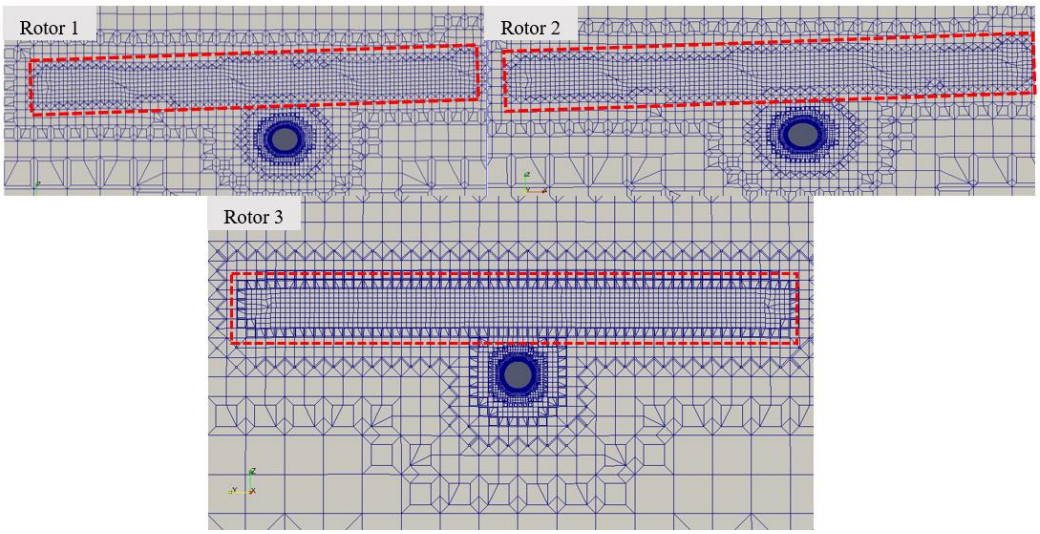

Fig. 35. Longitudinal mesh section of rotor disk

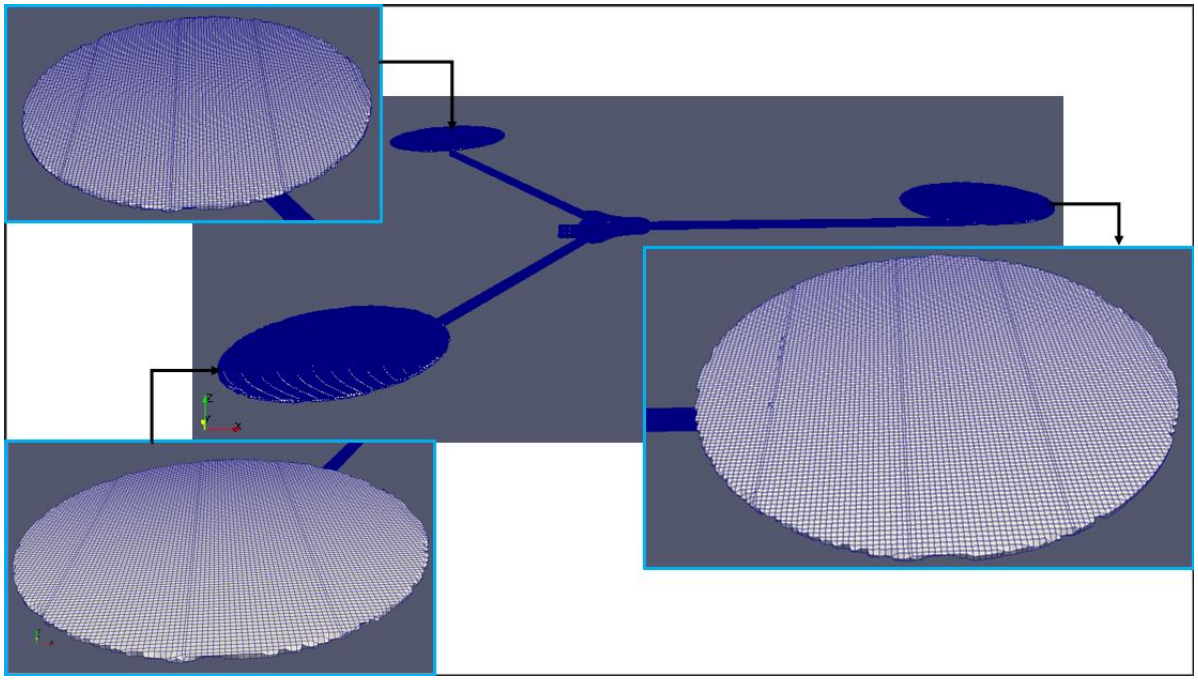

Fig. 36. Mesh configuration of rotor disk

Similarly, to the mesh generation described in Section 3.2, for the forward flight simulation of the full tri-copter model with rotating propellers, the y^+ value is also set at 2 corresponding approximately to the first layer thickness of 2.9 x 10^{-5} m. Y^+ distribution given by simulation reveals the same trends as section 3.2. Most of y^+ value on tri-copter is less than 1, average value of 0.67 for whole tri-copter. The minimum value of y^+ is 0.12 and the maximum value is 24.47.

5.4 Turbulence Model and Boundary Conditions

In CFD simulation, the simulation models of this paper used the k-ω SST turbulence model to simulate fluid flow. At Reynolds number 16315, the k-ω SST turbulence model is suitable for our study because this model has combined advantages of two turbulence models that are k-ε and k-ω [9].

The initial values of turbulent kinematic energy (k) and turbulence specific dissipation rate (ω) are [15]

$$k = \frac{3}{2} \times (UI)^2 = \frac{3}{2} \times (15 \times 0.02)^2 = 0.14 \ (\text{m}^2/\text{s}^2) \tag{15}$$

$$\omega = \frac{k^{0.5}}{C_\mu^{0.25} \times l} = \frac{0.135^{0.5}}{0.09^{0.25} \times 0.07 \times 1.33} = 7.21 \ (1/\text{s}) \tag{16}$$

CFD simulation used the k-ω SST turbulence model. Therefore, the boundary condition is set for three boundary areas in Figure 33 including: inlet (typed velocity inlet condition), outlet (typed pressure outlet condition) and tri-copter (typed wall condition). The quantities need to be established for the three regions in the k-ω STT turbulence model including: p (pressure), k (turbulent kinetic energy), nut, ω (turbulence specific dissipation rate) and U (velocity).

5.5 Results for Tri-Copter Simulation in Forward Flight

5.5.1 Residual convergence for forward flight simulation

Tri-copter is simulated in a rectangular computational domain with 15-m/s of forward speed. Convergence parameters of simulation problem are described in Table 7.

Table 7
Convergence conditions for simulation

Parameter	p	k	nut	ω	U
Convergence criteria	10^{-4}				
Under-relaxation	0.3	0.6			

Computational resources are used for total execution time (as shown in Table 8).

Table 8
Computer systems for simulation

System	Detail
High Performance Computing – HPC of HCM City University of Technology	- RAM: 128GB - Intel(R) Xeon(R) CPU E5-2680 v3 @ 2.5GHz x 48
Computer systems of HCMUT Department of Aerospace Engineering	- RAM: 16GB - Intel Xeon Processor E3-1225 v5 3.3GHz x 4

Figure 37 shows the convergence for the simulation of the tri-copter with three rotating propellers in forward flight. Calculating for the structured fined grid of about 16.6 million cells, the simulation was finished after 10000th iteration.

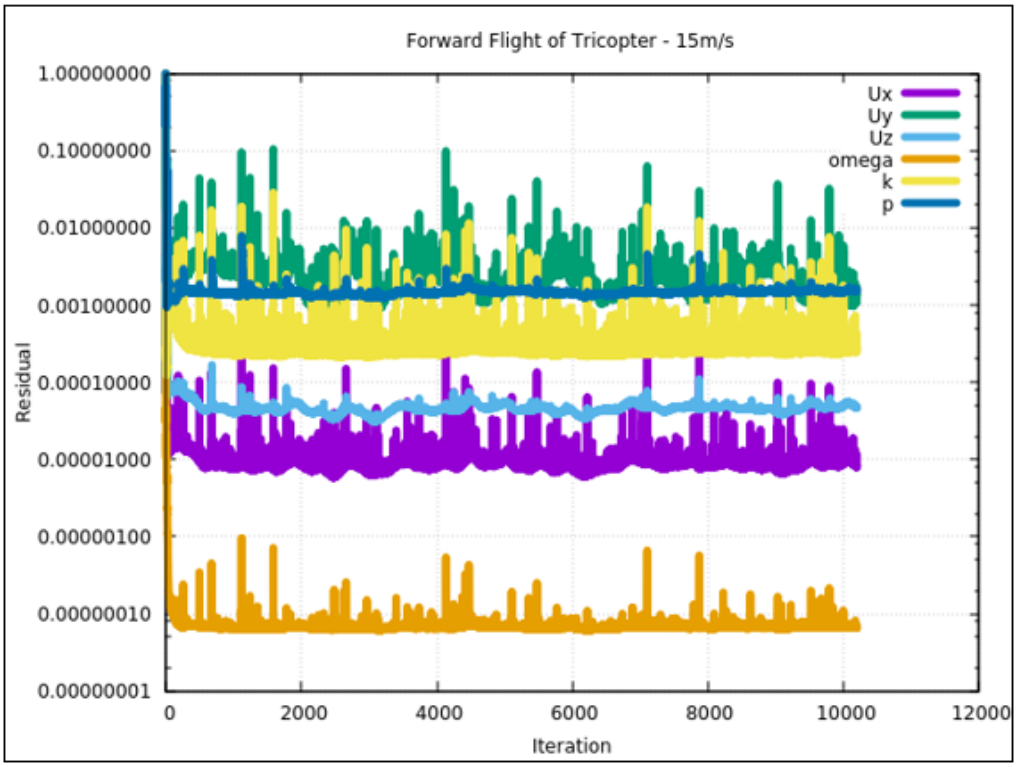

Fig. 37. Residual curves of forward flight simulation

As mentioned in Table 7, the convergence criterion was set 10^{-4}. It is obviously difficult to achieve higher or at least the same accuracy for the case of tri-copter's arm alone (without propellers) in Section 3. Residuals of all variables appear to be averagely stable after 10000 iterations. The turbulence specific dissipation rate - ω, velocity - U_x and velocity - U_z achieved residual error below 10^{-4}. Meanwhile, pressure - P, turbulent kinetic energy - k and velocity - U_y have their residual values stabilizing between 10^{-2} and 10^{-3}. As previously stated in section 5.3, due to complex 3D geometry of the tri-copter with the virtual disks representing the propellers, some defaults in boundary layer grid relating to y^+ value are unavoidable. This fact probably accounts for the high residual errors for the current simulation. However, the validation results presented in section 5.5.4 shows reasonable overall drag and thrust compared to those of the analytical approach based on BET and the thrust data from the manufacturer. The flow fields analysis from the simulation results of the airflow over the tri-copter with three rotating propellers at 4732-RPM and forward speed of 15-m/s can be considered appropriate, to some extent.

5.5.2 Velocity field on the rotor

The characteristic of airflow going through rotor in forward flight is "tip vortices" at around 90 and 270 rotor azimuth degrees. Azimuth angle, ψ, is used to define the blade position of rotor, which is defined as zero when the blade is pointing downstream, shown in Figure 38. These vortices often extend behind the rotors and the airflow is accelerated when passing through them.

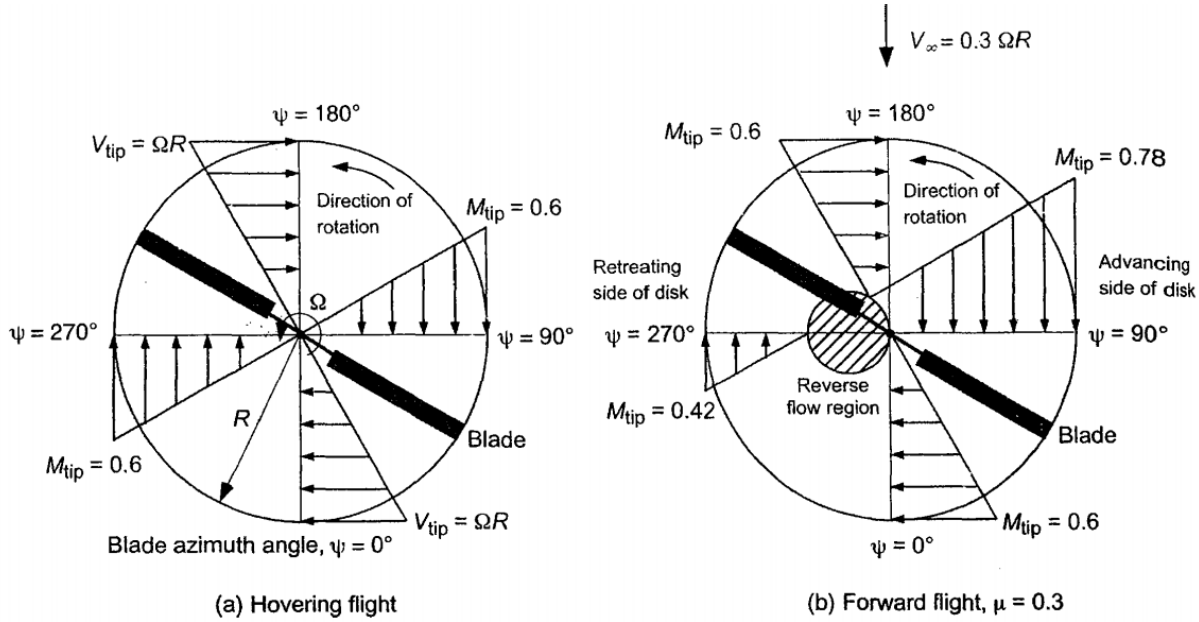

Fig. 38. Azimuth angle of rotor [8]

Velocity field on the rotors of tri-copter

i. In Figure 39, depending on the rotation direction of the rotor, the velocity field on the disk tends to be different. For Rotor 1 and Rotor 3 due to the same positive rotation, the velocity field on the disks are almost the same. In contrast, with Rotor 2 because of negative rotation, the velocity field tends to reverse when compared to Rotor 1 and Rotor 3.
ii. The red circle is the area where the airflow is accelerated after passing through the rotor. It is observed more clearly by looking at velocity vectors in Figure 40. In this region, the velocity of the airflow can reach nearly 20-m/s.
iii. The black circle is predicted to be the reverse flow area. This area locates on the retreating side of rotor. On rotor's blade, air travels from the trailing edge to the leading edge of blade profile.

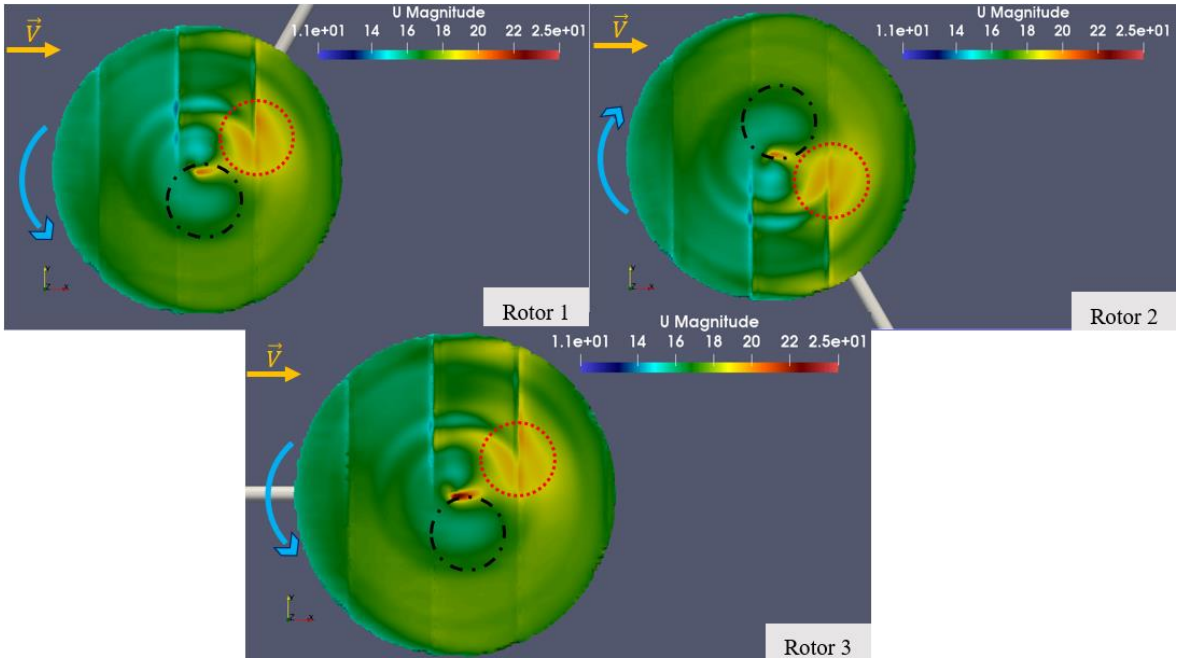

Fig. 39. Velocity field for rotors of tri-copter

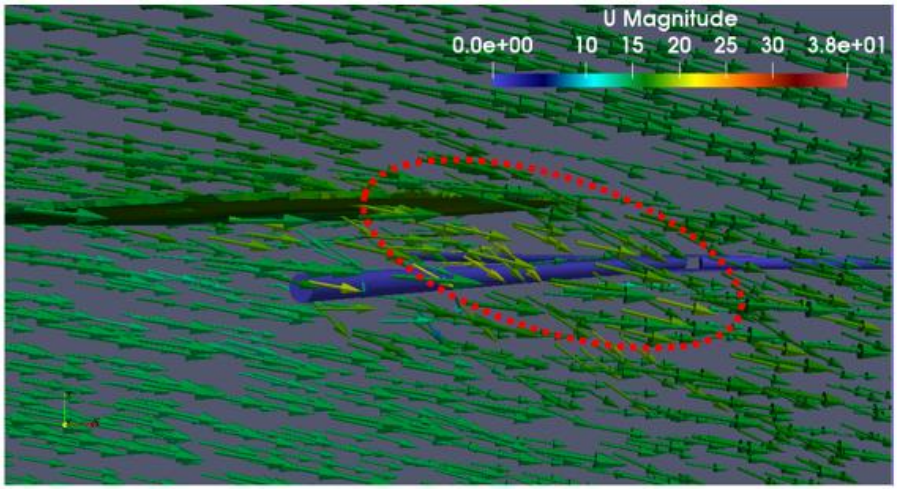

Fig. 40. Velocity vectors of airflow through rotor disk

In addition, the "tip vortices" of airflow when going through the rotor also occur in all three rotors of tri-copter. However, depending on the rotation direction of the rotor, these swirling locations are different (as shown in Figure 41).

Besides, the operation of the rotor also affects the fluid flow going through tri-copter. Figure 42 shows the streamlines of airflow. We see that the airflow is twisted when going through rotor disks, no longer as straight as before. Moreover, at the bottom position of Rotor 1 and Rotor 2, because of rotor operation, some streamlines move below the tri-copter's arm.

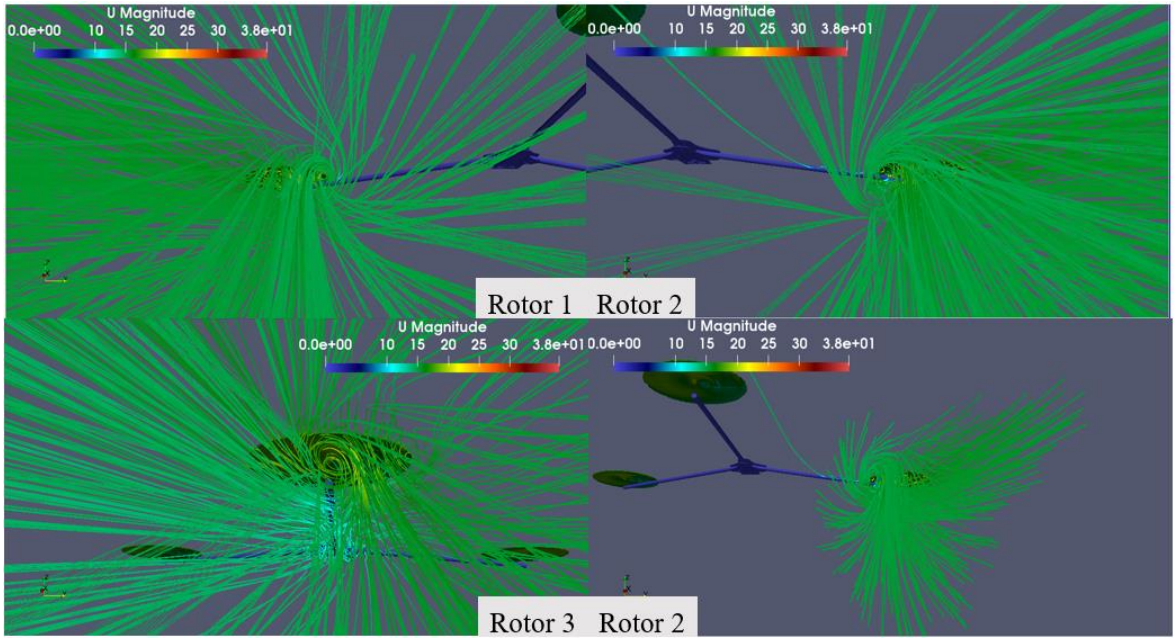

Fig. 41. Swirling streamlines of airflow through rotor disks

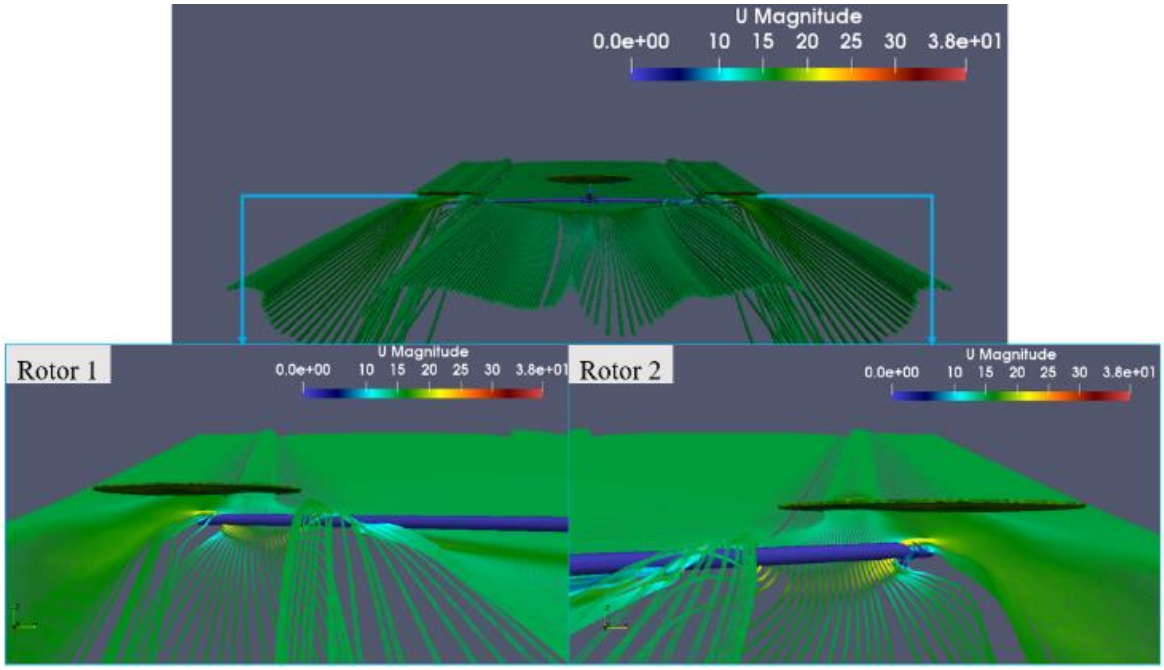

Fig. 42. Streamlines of airflow through tri-copter

5.5.3 Inflow ratio on the rotor

The inflow ratio is the dimensionless ratio for the induced velocity of rotor. This ratio is calculated according to the formula

$$\lambda_i = \frac{\upsilon_i}{\Omega R} \tag{17}$$

Figure 43 shows inflow ratio according to lateral coordinate of one rotor with small angle of rotor (α_{TPP} = -3^0) [13]. It is symmetrical across the axis of rotation. However, with large angle of rotor (α_{TPP} = -12^0), the inflow ratio is not symmetrical, illustrated in Figure 44 and Figure 45. This phenomenon is caused by reverse flow on retreating side of rotor (black circle).

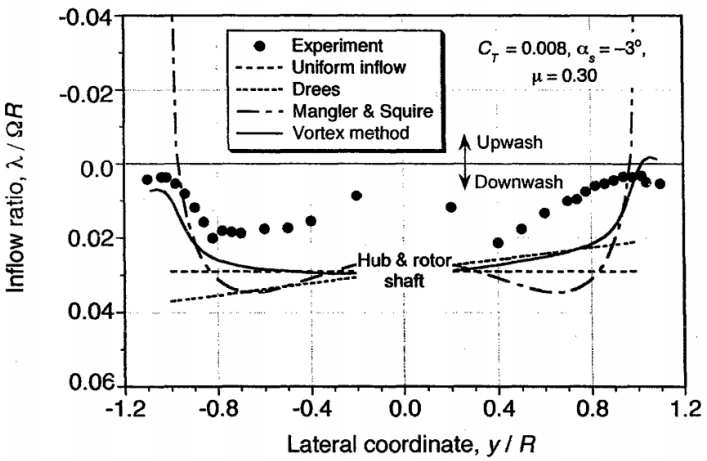

Fig. 43. Inflow ratio according to lateral coordinate on a rotor in forward flight with α_{TPP} = -3 degree [13]

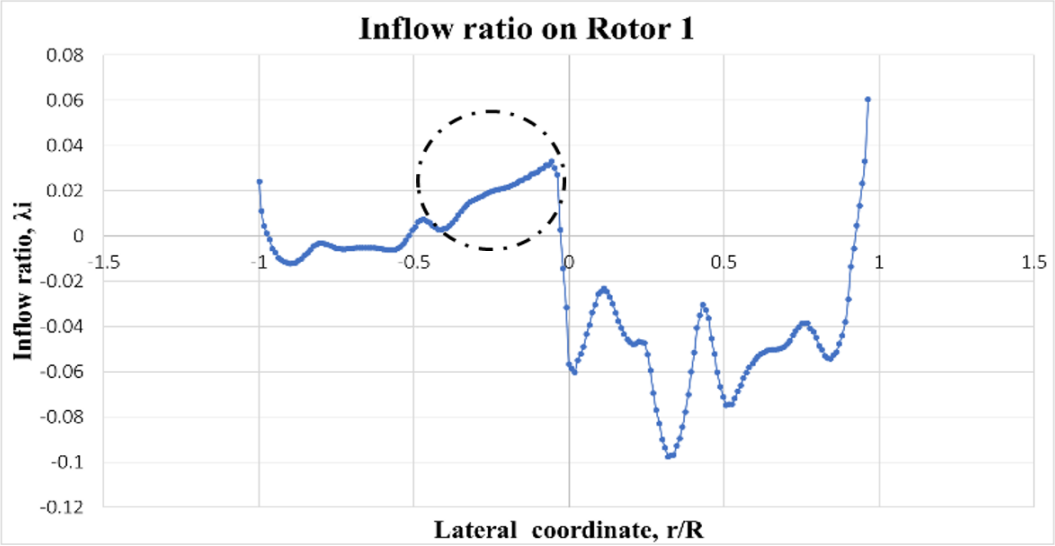

Fig. 44. Inflow ratio according to lateral coordinate on Rotor 1

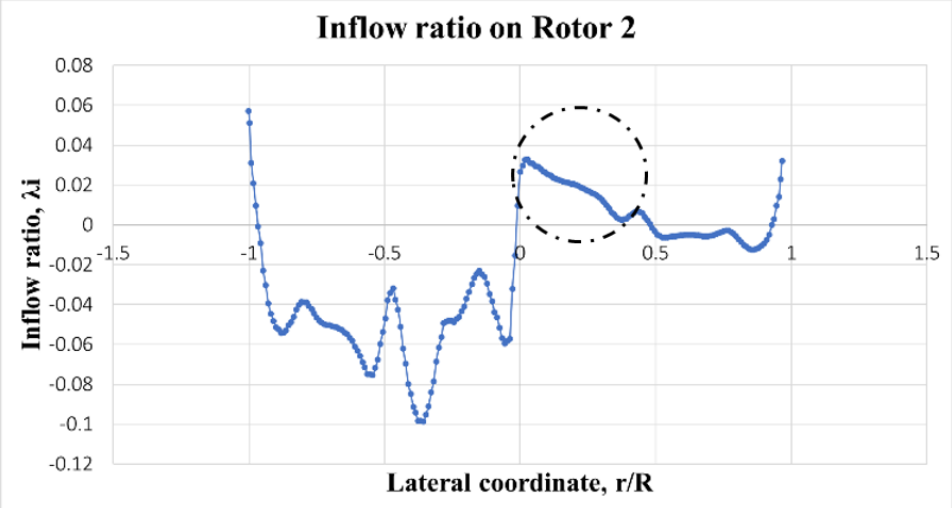

Fig. 45. Inflow ratio according to lateral coordinate on Rotor 2

5.5.4 Total thrust and drag of tri-copter in forward flight mode

Simulating tri-copter in forward flight is performed by two structural mesh (Table 9). Both structured meshes have initial y^+ value of 2.

Based on simulation results in OpenFOAM software, we have some results about total thrust and drag of tri-copter. To calculated total thrust of each rotor, we need to find effective angle of attack on rotor disk. Table 10 describes geometric angles of rotor disk from simulation results. At all three rotors, the maximum effective angle of attack is about -80 degree at root blade and the minimum effective angle of attack is about -7 degree at tip blade.

At 4732-RPM, each rotor must create 5.03-N of thrust. This value is calculated by analytical approach in Section 4. Beside thrust of rotor, in Section 4, we have the total drag of tri-copter that is 3.28-N. The analytical results are used to compare to CFD results. The simulation results were calculated from Mesh 1 (fined mesh) and Mesh 2 (coarse mesh). Table 11 shows results of two methods.

Table 9
Summary of two structural meshes

Parameter	Mesh 1	Mesh 2
Domain mesh	345 600	200 000
Final grid size	16 603 617	10 915 322
Hexahedral cell number	11 128 691	9 237 753
Cell number of rotor disk	- Rotor 1: 9180 - Rotor 2: 9180 - Rotor 3: 9123	- Rotor 1: 5324 - Rotor 2: 5324 - Rotor 3: 5312
Percentage of hexahedral cell	84.77 %	84.63 %
Skewness	3.88	3.34
Average non-orthogonality	8.26	8.64
Aspect ratio	25.04	30.02
Average layers	6.05	5.60
Total layers thickness	0.000581 (m)	0.000573 (m)
Coverage rates of layers	84.40 %	83.30 %

Table 10
Calculated geometric angles

Geometric angles of rotor (degree)			
	Throughout radius length (r/R_{rotor} from 0 to 1)		At 80% radius length
Rotor 1	From (at r/R_{rotor} = 0) to (at r/R_{rotor} = 1)	-79.96 -6.94	-8.60
Rotor 2	From (at r/R_{rotor} = 0) to (at r/R_{rotor} = 1)	-83.54 -7.01	-8.82
Rotor 3	From (at r/R_{rotor} = 0) to (at r/R_{rotor} = 1)	-81.35 -7.02	-8.82

Table 11
Calculated thrust and drag of tri-copter

Final Results from Two Approaches for Thrust (RPM = 4732)					
Rotor	Analytical Approach (BET)	Numerical Approach in OpenFOAM			
		Mesh 1		Mesh 2	
	Thrust (N)	Thrust (N)	Error (%)	Thrust (N)	Error (%)
Rotor 1		4.92	2.17	4.24	15.60
Rotor 2	5.03	4.92	2.02	4.29	14.67
Rotor 3		4.92	2.12	4.22	15.94
Manufacturer's specifications [9]: - Thrust = 5.10 (N) for propeller of RPM = 4732 -					
Final Results from Two Approaches for Drag of Tri-copter (RPM = 4732)					
	Analytical Approach (BET)	Numerical Approach in OpenFOAM			
		Mesh 1		Mesh 2	
	Drag (N)	Drag (N)	Error (%)	Drag (N)	Error (%)
Tri-copter	3.28	2.64	19.67	2.32	29.24

The "Error" parameters in Table 11 are different values between analysis result and simulation result, which calculated from formula:

$$Error = \frac{Numerical\_Approach - Analytical\_Approach}{Analytical\_Approach} \quad (18)$$

At 15-m/s of forward speed, the error for thrust of one rotor in Mesh 1 is approximately 2 %, and Mesh 2 is approximately 15 %. About total drag of tri-copter with three rotors, in Mesh 1, the error reach approximately 19 % and the error of Mesh 2 reach approximately 29 %. In conclusion, we see that the quality of Mesh 1 (fined mesh) is better than Mesh 2 (coarse mesh). With the above results, using virtual disks to represent the propellers in CFD simulation is a feasible approach. From comparison between simulation method, analytical method, and the thrust data from the propellers' manufacturer, the quality of simulation results is ensured.

6. Conclusions

The paper presents a through three-step-solving procedure including the analytical BET and the virtual blade method (VBM) integrating in the Reynolds-Averaged Navier Stokes solver in the open source code OpenFOAM. In this forward mode, the relative angle of -2 degree between the rotor tip-path-plane and the tri-copter's frame is calculated by BET method. Aerodynamic flow properties of the tri-copter in 15-m/s forward speed and three rotating propellers at 4732-RPM are achieved. Firstly, velocity field on rotors are showed. Depending on the rotation direction of rotor, the tendency of velocity field is different. Besides, the "tip vortices" of airflow due to gradient pressure between the top and bottom surfaces of rotor disk when it goes through rotors are illustrated by streamlines. In addition, airflow after going through rotors is accelerated, it can reach approximate 20-m/s. Secondly, the inflow ratio according to lateral coordinate is affected by reverse flow phenomenon on rotor disk. The influence makes inflow ratio not symmetry across the axis of rotation. Finally, based on the simulation results, the total thrust and drag of tri-copter are calculated. The results of simulation approach are compared to analytical approach to ensure simulation quality.

The results of this paper provide a methodological tool for the simulation of UAV-HOPE [1] – a flight vehicle combined fixed wing and three rotors in certain flights such as hover, climb and forward using VBM method. However, there are some limitations of the research. The residual errors for the forward flight simulation are still high, within the range 10^{-2} and 10^{-3} for three fundamental variables. Therefore, the mesh generation of the tri-copter need to be improved. In addition, the influence of tri-copter's frame to rotors activity is not considered and the torque is created by three rotors is not investigated. These are the research perspectives to be resolved in the next study.

Acknowledgement

The authors would like to send special thanks to Department of Aerospace Engineering and High Performance Computing Laboratory, Ho Chi Minh City University of Technology for providing facility and computational resources for this research.

References

[1] Huynh Tri PHAM. *Design a VTOL UAV – Stability and analysis & 3D simulation*, Thesis, Ho Chi Minh City University of Technology-Vietnam, unpublished, 2015.

[2] Alessandro Bianchini et al. "Potential of the Virtual Blade Model in the analysis of wind turbine wakes using wind tunnel blind tests", *72nd Conference of the Italian Thermal Machines Engineering Association*, Lecce, Italy, 2017.

[3] Filippone, A., J. P. Chollet, and J. Lewandowska. "CFD actuator disk solutions for a helicopter rotor in hover flight." *University J. Fourier of Grenoble, France and University of Manchester Institute of Science and Technology, UK* (2003).

[4] Wahono, Stefano. *Development of Virtual Blade Model for Modelling Helicopter Rotor Downwash in OpenFOAM*. No. DSTO-TR-2931. DEFENCE SCIENCE AND TECHNOLOGY ORGANISATION FISHERMANS BEND (AUSTRALIA) AEROSPACE DIV, 2013.

[5] Khanh NGUYEN, Thi Hong Hieu LE, Ngoc Hien NGUYEN. "Numerical simulation for Vertical Take-off and Landing UAV using Virtual Blade Model", *South East Asia Workshop on Aerospace Engineering - SAWAE*, Bangkok, Thailand, 2018.
[6] Khanh NGUYEN. *Numerical approach for vertical take-off and landing unmanned aerial vehicles (VTOL-UAV)*, Thesis, Ho Chi Minh City University of Technology-Vietnam, unpublished, 2018.
[7] Tran Anh Khoi NGUYEN. *Investigate the stable characteristics of tri-copter in automatic flight mode*, Thesis, Ho Chi Minh City University of Technology-Vietnam, unpublished, 2019.
[8] Adam Sieradzki. *Aeroelastic analysis of helicopter rotor using Virtual Blade Model and equivalent beam model of a blade*, Institute of Aviation, Department of Aerodynamics and Flight Mechanics, Poland, 2016.
[9] Thi Xuan Huynh TRAN. *Numerical simulation for hydrid UAV combined fixed-wing and propellers (HOPE)*, Thesis, Ho Chi Minh City University of Technology-Vietnam, unpublished, 2018.
[10] ANSYS Inc. *Introduction to ANSYS FLUENT*, 2010, available online: https://imechanica.org/files/fluent_13.0_lecture06-turbulence.pdf
[11] J. John Anderson. *Fundamentals of Aerodynamics*, 5th edition, The Mc-Graw-Hill Companies, New York, USA, 2011, pp.293.
[12] L. Sankar. *Steady – Level forward flight*, unpublished , 2002.
[13] J.Leishman. *Principles of helicopter aerodynamics*, 2nd edition, Cambridge University, New York, USA, 2006, pp.116-117.
[14] XOAR PJP T-L 1245 characteristics from manufacturer. available online: https://www.xoarintl.com/multicopter-propellers/precision-pair/PJP-T-L-Precision-Pair-Multicopter-Carbon-Fiber-Propeller-Low-Kv-Motor/#des
[15] Joel GUERRERO. *Introductory OpenFOAM Course*, University of Genoa, DICCA, 2014.